Engineering

Research

Early in the ideation phase, we have decided to improve on CAR T therapy due to its promising effect in hematological malignancies. To mount an effective and durable antitumor response, CAR-T cells must be able to infiltrate the tumor, recognize its cognate antigen, perform their effector function, then differentiate into memory cells that ensure long-term protection. Major obstacles to efficacious CAR T cell therapy in solid tumors is their intrinsic ability to escape from immunosurveillance through various mechanisms. To unleash its hidden potential in solid tumors, there are four major barriers that have to be overcome: immunosuppressive tumor microenvironment (TME), antigen heterogeneity, on-target-off tumor toxicity, and tumor antigen escape. Below are works that has already been done in the field of synthetic biology to address the four barriers:

a) Immunosuppressive tumor microenvironment

The migration of CAR T cells into solid tumor sites is inadequate to confer tumor elimination due to the highly dynamic immunosuppressive tumor microenvironment (TME). Chemokine-receptor binding is pivotal to CAR T trafficking to tumor sites. Thus, gene modification is done to CAR T cells to equip them with chemokine receptors to better respond to tumor-derived chemokines. CAR T cells overexpressing CXCR2 have shown enhanced infiltration and tumoricidal effect in hepatocellular carcinoma (HCC). Similarly, upregulated CXCR3 mediated homing of adoptively transferred CD8+ T cells and abrogated therapeutic benefits in melanoma. Identification of a chemokine-receptor axis suitable for therapeutic targeting is obscure due to the heterogeneity and non-uniform pattern of chemokine expression among different tumor types, which is a hurdle to prompt application of chemokine receptor incorporated CAR T cells.

b) Antigen heterogeneity

Safe and effective clearance of CAR T cells requires specific and reliable expression of antigens on the cell surface. A major challenge of CAR T therapy in solid tumors is the lack of amenable tumor-restricted CAR-targetable antigens. Unlike haematological malignancies, in which the cancer cells usually express a specific surface marker, it is more common to recognize a tumor-associated antigen on solid tumors. The tumor-associated antigens are also expressed in low levels in normal somatic tissues, augmenting on-target off-tumor toxicity. Fatal central nervous system toxicity has resulted from the administration of CAR T cells targeting GD-2 positive neuroblastoma. ERBB2 targeting CAR T treatment precipitated lethal lung toxicity in a patient with metastatic colorectal cancer. The occurrence of these catastrophic adverse events from non-specific antigens highlights the significance of identifying a safe antigen confined to tumors.

c) On-target-off-tumor toxicity

Nonetheless, identifying antigens that are exclusively expressed on the tumor cell surface is a key challenge to translating CAR-T treatment in solid tumors into clinical prospects. Due to the heterogeneity of solid tumors, CAR T cells targeting a single antigen may result in tumor recurrence due to excessive growth of antigen-negative cells or cells expressing low antigen levels. To improve antigen recognition, bispecific CAR T cells that could recognize two antigens present on tumor cell surface simultaneously are engineered. The transgene of the bispecific antigen recognizing extracellular domain is introduced to T cells isolated from patients by retrovirus transduction. Studies reveal CAR T cells co-expressing CD19 and HER2 exhibit greater antitumor activity than CAR T cells with a single target. It has been shown to preserve cytolytic ability upon loss of one of the targeting antigens, reducing the probability of escape from CAR targeting through antigen loss. Bispecific CAR T cells, however, potentially further off-tumor cytotoxicity due to multiple non-tumor specific targets. Researchers turned to introduce antigens to tumor cell surface as CAR targets. Park et al. used an oncolytic chimeric vaccinia virus to deliver a non-signaling variant of CD19 to tumors as CAR target. This approached is coined with the term 'tumor-tagging'. Subsequent incubation of the CD19t expressing tumor cells with CD19 CAR T cells has demonstrated CAR T cell activation and tumor killing ability in vitro, and a significant reduction of tumor volume in mice engrafted with subcutaneous breast adenocarcinoma. Limitations of such an approach are the restricted persistence of immunogenic vaccinia virus due to humoral immune clearance and off-tumor cytotoxicity directed to CD-19 positive B cells.

d) Tumor antigen escape

Insufficient activity of CAR T cells due to low antigen density has emerged as an important cause of cancer relapse and recurrence. CAR T cell potency is highly dependent on target antigen expression, and subthreshold antigen levels are often associated with failure in exerting significant anti-tumor activity. As evidenced in a clinical trial testing CD-22 targeted CAR T cells for patients with refractory B-ALL, complete tumor remission was tempered by frequent relapses driven by subthreshold antigen levels. Both gain-of-function and loss-of-function models illustrated upregulation of specific antigens is central to the curative effector function of CAR T cell treatment. Studies have been focused on tuning the antigen density requirement for CAR T activity. CARs coupled to CD28 co-stimulatory domain is introduced to T cells by retroviral vectors and has shown to be less susceptible to antigen downregulation in HCC. Subsequent studies revealed GPC2-CAR T cells expressing c-Jun and with CD28 co-stimulator endo-domains lower the antigen density threshold by 10-folds. Of note, for shared antigens that are expressed at lower levels on normal tissues, on-target off-tumor toxicity will be exemplified, which poses challenge to modulation of CAR T sensitivity to antigen threshold.

Part 1: Construct design

Design

a) Tumor-tagging

As our literature review highlighted the profound impact of tumor microenvironment, antigen heterogeneity, and antigen density on the potency of CAR T, we have decided to work on each and every aspect to improve CAR T therapy. After reviewing academic journals, we have decided to work on the idea of tumor-tagging. Instead of identifying a suitable antigen, tagging tumor cells broadens the spectrum of antigen available as CAR target. Previous scholars delivered truncated CD19 as CAR target, which will cause B cells dysplasia inevitably. A recent research reveals CD19 might also be present on surface of mural cells, hence neurotoxicity might be a potential adverse effect caused by CD19 CAR T cells. Therefore, we aim to choose an CAR target that will not be found on normal human cells, which is at the same time immunogenic, enable elimination by host immune responses in addition to cytotoxic effect of specific CAR T cells.

b) iGEM15 Evry Entrepreneur

The team iGEM15 Evry Entrepreneur worked on the expression of a novel antigen, OVA1, on the membranes of S. cerevisiae. The tumour antigen OVA1 was fused to DEC205 scFv, a lectin receptor expressed by certain subsets of dendritic cells (DC), including mouse spleen DC. This structure was anchored by AGA2p, which is a component of their surface display system. This group has successfully transformed yeast to display high levels of antigen on the surface of DC via AGA1P. In addition, this chassis was able to induce the DC with an increase in CD80/CD86 and MHCI/MHCII in all transformed yeast relative to wild-type yeast. Furthermore, their in vivo study revealed that vaccination with yeast OVA1-DEC205/OVA2 resulted in a significant CD8+ OVA1 induction compared to PBS control and wild-type yeast. Thus, their group came to the conclusion that this chassis is able to generate a high antigen load to elicit a rigorous immune response. Their group has demonstrated the feasibility of introducing a foreign antigen onto the surface of DC through a MHC-I-restricted pathway, which stimulates CTL killing of nearby tumour cells.

c) Hepatocellular carcinoma

Once optimized, the tumor tagging system could be applied to every solid tumor. Within the course of the iGEM competition, it is impossible and impractical to exhibit the efficacy on every tumor type. We have chosen hepatocellular carcinoma as it is one of the most studied tumor types for CAR T application solid tumors.

HCC is the most common primary liver cancer, usually diagnosed at an advanced stage. Current management options for HCC remain limited. Although previous studies have indicated the feasibility of CAR-T cells, like in other solid tumors, ideal therapeutic effects are yet to be achieved. Our system, thus, aim to improve the efficacy of CAR-T cells in HCC.

d) Adeno-associated vector

Previous attempts used oncolytic virus as a vector for antigen transgene delivery. Our PI expressed concern over whether the antigen could be sythesized and expressed stably if the oncolytic virus attacks the tumor cells. Hence, we borrowed the idea from gene therapy, using one of the most characterized vectors used in *in vivo* gene therapy – recombinant adeno-associated virus (rAAV).

Upon administration, the rAAV will be recognized by the host's cell surface receptor, which triggers endocytosis of the rAAV. The single stranded AAV (ssAAV) undergoes endosomal escape, trafficking into nucleus, uncoating, and proteolysis by the proteasome. In the nucleus, the transcriptionally inert ssAAV undergoes second strand synthesis to be converted into a double-stranded, and transcriptionally active form. The viral inverted terminal repeats (ITRs) in the rAAV genome could drive recombination to form circularized episomal genomes that can persist in the nucleus, with a low frequency of insertion into the host genome. rAAV is deemed as an ideal vector for in vivo transgene delivery due to its low pathogenicithy, minimal immunogenicity, low risk of insertional mutagenesis, and ability to infect both dividing and non-dividing cells, as compared to other viral vectors used in transgene delivery, including adenovirus, herpes simplex virus (HSV), retrovirus, and lentivirus.

To date, there are 12 AAV serotype discovered and over 100 variants. Different serotypes have tissue tropisms. For our treatment, AAV2 is proven to possess natural preference of AAV2 vectors for HCC compared to non-malignant liver cells in mice and human tissue, due to the improved intracellular processing of AAV2 vectors in HCC. AAV2 exhibited enhanced transduction efficiency in HCC, independent of the promoter and transgene. Being one of the two AAV vectors receiving regulatory approval for commercial use on patients, AAV2-based platforms for transgene delivery is also the most numerous in clinical trials.

The major limitation of rAAV vector is its small cargo capacity of 4.7kb. Due to the insert length restriction, the payload but be meticulously designed to consider not only therapeutic transgene, but also essential regulatory sequences, like Woodchuck Hepatitis Virus Posttranscriptional Regulatory Element (WPRE) (BBa_K4469002), and hGH polyA (BBa_K404108).

Based on our research, we have decided to design an rAAV2 vector for tumor tagging, as well as to tackle each and every obstacle that CAR T cell therapy faces. In general, we envision the rAAV vector that we have to build could achieve the following goals:

1. Tumor-specific expression of an immunogenic
2. Upregulate MHC Class 1 expression
3. Increase CAR T infiltration
4. Short length of coding sequence

e) Antigenic peptide – SIINFEKL

To allow effective tumor-tagging and CAR T-cell recognition, SIINFEKL sequence is included in the vector. OVA (257-264) SIINFEKL codes for chicken albumin peptide that could be presented by MHC class I complex. OVA is selected for its non-human origin, thereby reducing the on-target off-tumour effects caused by conventional CAR-T therapy, which targeted antigens that could be found in both healthy and tumor cells. In addition, SIINFEKL can induce cytotoxic T lymphocyte (CTL) response. Following CD8+ cytotoxic T cell recognition of the epitope, TNF-α and IFN-γ secretion promote activation and proliferation of naïve and effector T cells. A previous study has shown the feasibility of engineering CAR T specific for ovalbumin (OVA) peptide SIINFEKL. They demonstrated that the OVA protein improved in vivo T cell proliferation and inflammatory cytokine secretion and concluded that this is a way to enhance CAR T-cell efficacy for solid cancers. SIINFEKL will be loaded onto the MHC Class I directly, bypassing the normal antigen presentation pathway, in which the section of the peptide to be presented cannot be controlled. As the hepatocellular carcinoma cells are coated with SIINFEKL, it is susceptible to killing by CAR-T designed with receptor targeting it.

f) miRNAs

Since rAAV optimally accommodates genomes under 4.7kb, it is not uncommon to use RNA interference as an alternative to protein-coding genes for its shorter sequence. Micro RNAs (miRNAs) are our target as some pro-inflammatory miRNAs are often downregulated in tumors. Mature miRNAs are 20-24 nucleotides long. With 100nt flanking sequence on both the 5' and 3' end of the miRNA sequence for miRNA biogenesis, it will take only up to around 200bp on our insert, which is favourable to an AAV vector.

Upregulation miRNA26a (BBa_K4469007) is well appreciated in AAV-based gene therapy for HCC. It is the first remarkable miRNA gene therapy using AAV vector. While downregulation of miR26a is correlated with HCC recurrence, metastasis and poor prognosis, gain-of-function test also verified it's ability to suppress tumour growth, invasion and metastasis of HCC, *in vitro* and *in vivo*. Aside from its direct tumor-suppressive nature, it could also achieve one of our therapeutic goals - enhance the CAR T infiltration, by promoting immunoenhancing chemokines expression. Interleukin-6 (IL-6) is one of the major downstream targets of miR26a. IL-6 blockade could enhance CD8+ T cell recruitment to boost the anti-tumor immunity. Increased IL-6 secretion by tumor cells would activate the STAT3 pathway in $CD4^+$ T cells and myeloid cells, and stimulate the differentiation of $CD4^+$ T cells into IL-4-producing Th2-like cells rather than IFN-γ-producing effector Th1 cells. IFN-γ was also proved to boost the production of the chemokines CXCL9 and CXCL10 by tumor-localized myeloid cells to facilitate the migration of CXCR3+ NK and CD8+ T cells towards the tumor. Therefore, using the miRNA-26a which can suppress the IL-6 expression in liver tumor cells, would help establish a positive feedback loop and lower the impact of the tumor environment for CAR-T infiltration.

To increase MHC class I level for antigen expression, miR28 (BBa_K4469008), which is known to be a tumor suppressor of hepatocellular carcinoma, will be encoded. MHC class I downregulation is one of the significant causes of tumor escape, which occurs in more than

40% of human cancer tissues. As the SIINFEKL peptides are selectively presented by MHC class I, downregulation of the complex will result in ineffective antigen presentation. Therefore, increasing the MHC-I level is needed to express the antigen of interest. miR 28 is an inhibitor of N4BP1. N4BP1 prohibits the activation of NFkB by competitive binding for polyubiquitin with NEMO. Inhibition of NFkB results in downregulation of MHC class I molecules. Due to the antagonistic ability of N4BP1, we could upregulate NFkB and hence the MHC class I.

g) iGEM15 BGU Israel

The BGU Israel selected AAV to transport their system to the body. Using hTERT as a cancer-specific promoter, their system also generated exogenous proteins that may identify tumors for simpler surgical removal, leading to cancer cell death and by acting as a biomarker for blood or urine cancer detection. BGU Israel has shown the practicability of gene therapy that specifically acts on tumor sites or cancer cells to prevent off-target effects.

h) Tumor-specific promoter

From BGU Israel and other literature on AAV gene therapy, we learnt that the tagging selectivity could be ensured by tumor-specific promoters. In our study, we will ensure the tagging selectivity by employing 3 tumor-specific promoters.

To ensure tumor-specific expression of the our antigenic peptide SIINFEKL, a2bM, composed of 2 enhancers A (E_A), enhancer B (E_B), and HCC-specific alpha-fetoprotein (AFP) promoter is selected (BBa_K446900). The specificity of this AFP promoter variant is assessed by the AFP expression level in various cell types: AFP-positive HCC (Huh7, HepG2, and Hep3B), AFP-negative HCC (HepI), non-HCC cancer cells (U343 and A549), and normal fibroblasts (BJ, W138, and IMR90). a2bM selectively induced expression of luciferase in all AFP-positive HCC cells, while minimal to no luciferase activity is observed in AFP-negative cells and normal cells. This shows that the promoter variant can express genes specifically in AFP-positive cancer cells, minimizing the off-target effects on functional hepatocytes. Moreover, this promoter demonstrates a more robust induction of transgene expression than entire-length human AFP. This could be due to the removal of the silencer in the a2bM variant, which helped enhance the transcriptional activity of AFP promoter without compromising its specificity. In AFP-positive HCCs, transcription would be activated, and transgenes are shown to be expressed 43- to 456-fold higher than in cells with AFP promoter lacking the enhancers. Therefore, a2bM-AFP is inserted into the vector to allow HCC-specific transcription and enhance transgene expression in AFP-positive HCC.

To drive tumor-specific miRNA expression, two human telomerase reverse transcriptase (hTERT) promoters (BBa_K1722002) are included. Overexpression of TERT is observed in about 90% of cancers (in contrast to <20% in normal cells) and contributes to HCC carcinogenesis by increased TERT-mediated telomerase maintenance. Gene expression analysis making use of qRT-PCR has proven a higher (over 10 to 50-fold) TERT mRNA expression in HCC tissues compared to background, non-tumor liver tissue, and normal liver tissues. The specificity of this promoter is assessed by the fluorescence intensity in normal

(HEK293T) and HCC (HepG2) cells, and it is shown that hTERT owns a much higher expression ability in HCC cells compared to normal cells, as characterized by iGEM21 ZJU CHINA.

i) How did we build upon existing iGEM teams?

We will demonstrate the possibility of employing a rAAV2 vector to express a novel antigen OVA on tumor cells, based on the discoveries of earlier iGEM teams. Expression on tumor cells is a more direct method of inducing cytotoxic T-lymphocyte (CTL) than expressing antigen on DCs, as iGEM15's Evry Entrepreneur accomplished. Antigen-tagged tumor cells may be targeted more readily. Interferon gamma (IFN-g) is incorporated into their design in order to overcome the immunosuppressive environment established by cancer cells and to induce the development of MHC-I and MHC-II on DCs, leading to the activation of T-Cells. Indeed, the anti-tumor effects of IFN-g have contributed to the success of current cancer immunotherapies. Nonetheless, a significant proportion of patients exhibit primary resistance to these therapies, and further immunotherapy relapse reports are beginning to emerge. Within immunogenic or inflammatory tumor microenvironments, a persistent presence of IFN-g does not contribute to the eradication of tumor cells by its "bright side" function, but rather induces the selection and production of tumor clones with a more malignant phenotype by its "dark side" function. In addition, studies have demonstrated that the IFN- response of tumors plays a crucial role in determining the susceptibility of tumors to immunotherapies, which can potentially contribute to the development of acquired immunotherapy resistance. Given that OVA peptides are selectively presented by MHC class I, our group's approach takes advantage of the function of miRNAs in which miR 28 is utilized to boost MHC class I level for antigen production. Additionally, miR 26a is introduced into the ATREUS vector to increase CAR T infiltration by stimulating the production of immunoenhancing chemokines in an effort to overcome the immunosuppressive environment of solid tumors. ATREUS will demonstrate the effects of miRNAs in the combination of gene therapy and immunotherapy, which is still a relatively new and unexplored field.

hTERT promoter is a well characterized part in iGEM's Part Registry, previously employed by iGEM15 BGU Israel, iGEM18 CPU CHINA, iGEM21 ZJU China, and some other teams. We will demonstrate the feasibility of expressing 2 miRNA transgenes, miRNA-28-5p and miRNA-26a, which were not investigated by previous iGEM teams, utilising the hTERT promoter. In addition to the well-known hTERT, we will expand the impact of prior iGEM teams and increase the specificity of our system by incorporating hTERTs and an unexplored tumor-specific promoter, a2bM-AFP. It is composed of 2 enhancers A (E_A), enhancer B (E_B), and an alpha-fetoprotein (AFP) promoter that is specific to HCC. Using three cancer-specific promoters, similar to the design of BGU Israel, we assure that our system will be activated exclusively in cancer cells, with minimal expression, if any, in healthy cells. Simply by modifying the vector components to match the microenvironment of each patient's tumor, our modular system can be redesigned to accommodate the specific attributes of each malignancy.

j) Design of target plasmid

The plasmid map below is the rAAV target plasmid our team designed. SIINFEKL is flanked by Internal ribosome entry site (IRES) (BBa_K4469009) on the 3' end. IRES could be used for second gene expression under the same promoter in a cap-independent manner. Enhanced green fluorescent protein (EGFP) (BBa_E0040) on the 3' end of IRES sequence serves as a reporter to display the activity of a2bM-AFP promoter, and subsequently transfection and/or transduction efficiency.

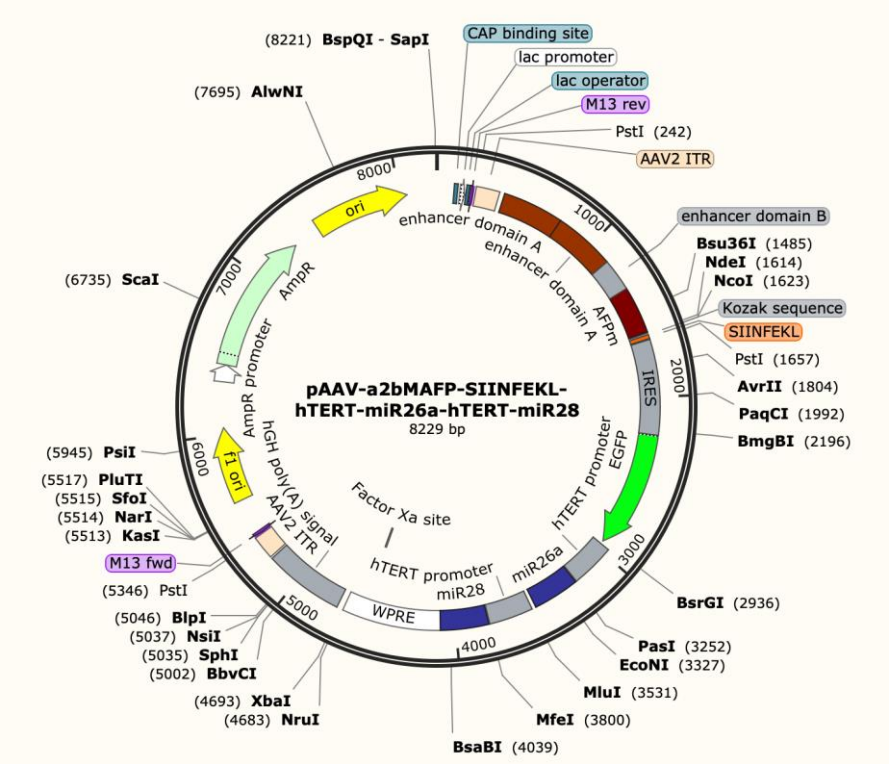

Figure 1 Plasmid map of pAAV-a2bMAFP-SIINFEKL-hTERT-miR26a-hTERT-miR28

k) Design of control plasmid

As we have proposed a novel approach of AAV-based tumor-tagging, it is of utmost importance to examine the specificity and activity of the tumor-specific to guarantee the safety and effectiveness of our proposed system. A control plasmid would have to be cloned to compare the transgene expressions by tumor-specific promoters against universal promotes in both cancer and HCC cell lines.

Human cytomegalovirus (CMV) promoter (BBa_I712004) is an extensively characterized constitutive promoter in mammalian cells. Its immediate early enhancer/promoter activity was consistently the highest in mammalian tissues. The CMV promoter with immediate enhancer will be used to drive the expression of SIINFEKL and EGFP, as a comparison to a2bm-AFP promoter to demonstrate the tagging selectivity.

U6 promoter (BBa_K2200003) is one of the promoters that are used to drive the expression of small RNAs in mammalian cells. In a study of the Type 3 RNA polymerase 3

promoters, it is shown that U6 promoter has the highest efficiency in driving the transcription of luciferase in human cell lines. Expression of miR26a and miR28 will be driven two U6 promoters, as a comparison to hTERT promoter to ensure tumour-specific transcription of miRNAs.

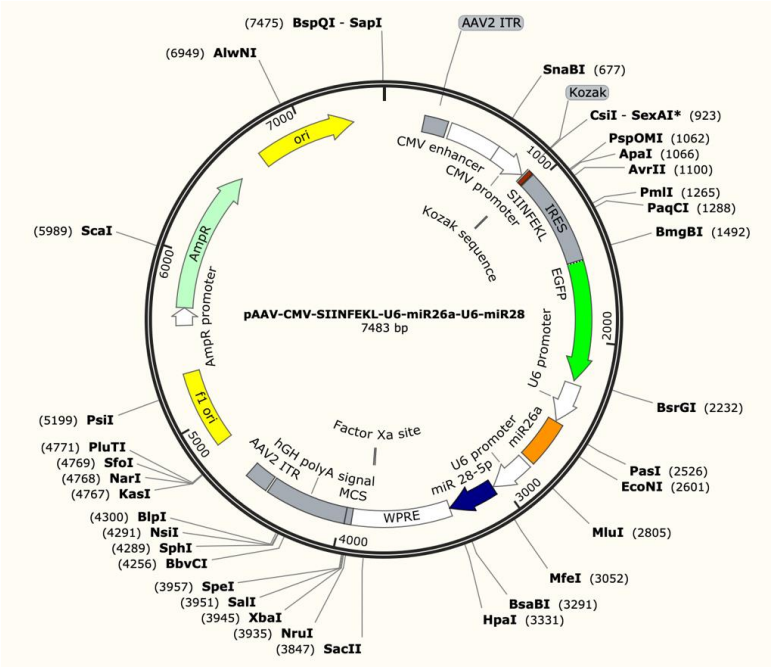

Figure 2 Plasmid map of pAAV-CMV-SIINFEKL-U6-miR26a-U6-miR28

Build

a) Target plasmid (pAAV-a2bMAFP-NLVPMVATV-hTERT-miR26a-hTERT-miR28) cloning

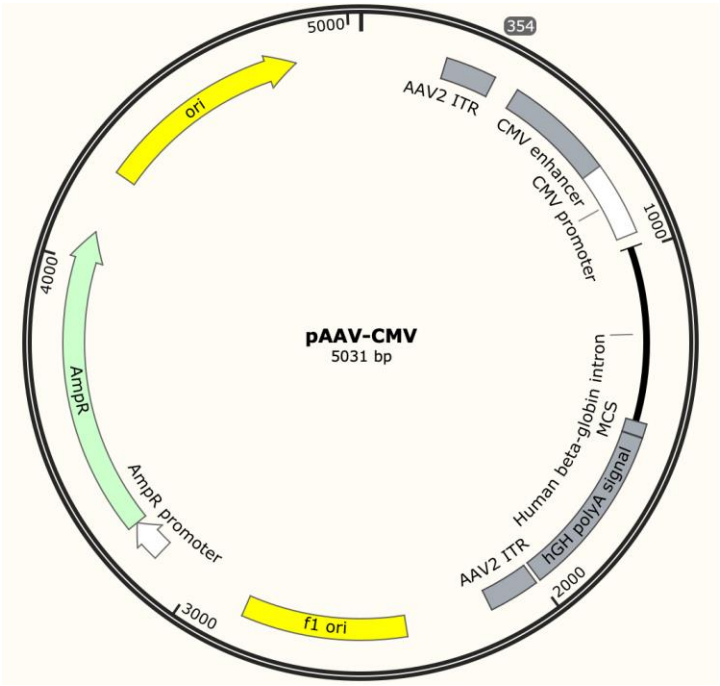

Figure 3 Plasmid map of pAAV-CMV

The rAAV2 backbone of transfer plasmid is obtained from Takara. Insert (BBa_K4469016) synthesis performed by Genscript, then subcloned into the AAV2 backbone at between the 387bp and 1502bp of the backbone. Next Generation Sequencing is performed by Genscript for sequence verification.

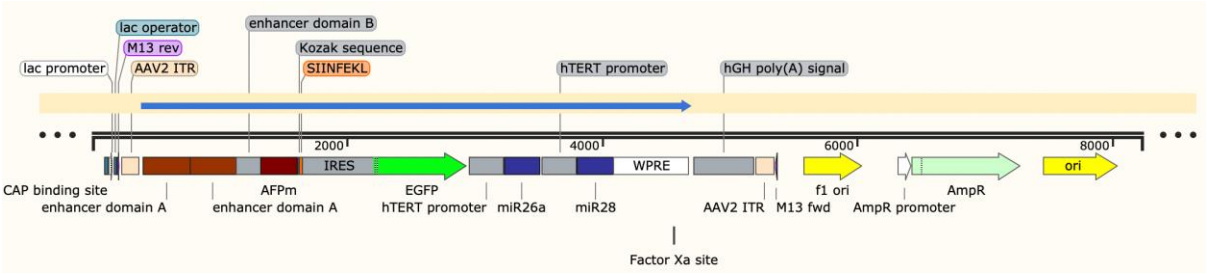

Figure 4 Next Generation Sequencing result of pAAV-a2bMAFP-SIINFEKL-hTERT-miR26a-hTERT-miR28

The verified pAAV-a2bMAFP-SIINFEKL-hTERT-miR26a-hTERT-miR28 plasmid is transformed into One Shot™ Stbl3™ Chemically Competent *E. coli* cells from Invitrogen. 1ng of plasmids were incubated with 50ul Stbl3 and heat shocked at 45°C for 1.5 minutes. Transformed bacterial cells are plated on LB agar plate with Ampicillin. Colonies were grown after overnight incubation at 37°C. Successfully transformed *E coli*. cells form white colonies on the plate.

Figure 5 Bacterial colonies of transformed pAAV-a2bMAFP-OVA-hTERT-miR26a-hTERT-miR28

Colonies are picked and grown in Ampicillin containing LB medium overnight. Maxiprep is performed to extract the transfer plasmid using kit from Qiagen, then sent to Tech Dragon Limited for Sanger sequencing.

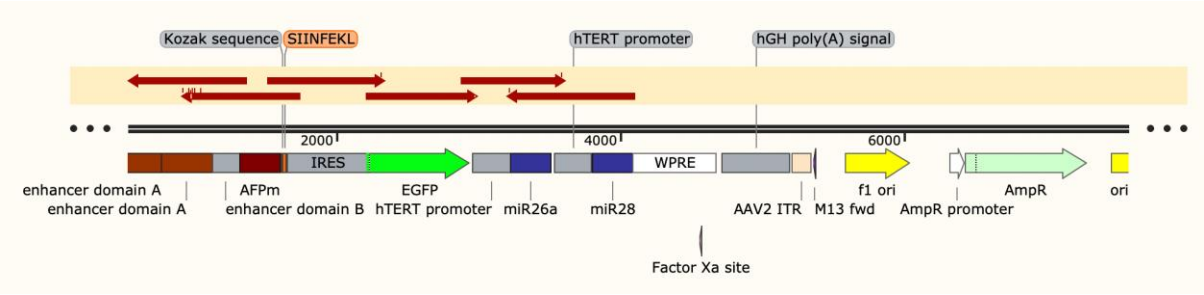

Figure 6 Sanger sequencing result of the pAAV-a2bMAFP-SIINFEKL-hTERT-miR26a-hTERT-miR28 after Maxiprep

b) Control plasmid cloning

5 gene fragments (CMV, SIINFEKL, IRES-eGFP, U6-miR26a, and U6) are obtained from Integrated DNA Technologies (IDT). They are amplified by standard polymerase chain reaction (PCR) using the following system and program:

	CMV	**SIINFEKL**	**IRES-eGFP**	**U6-miR26a**	**U6**
ddH_2O	20 ul	20 ul	20 ul	20 ul	20 ul
2x Phanta Flash Master Mix	25 ul	25 ul	25 ul	25 ul	25 ul
Forward primer (10uM)	2 ul	2 ul	2 ul	2 ul	2 ul
Reverse primer (10uM)	2 ul	2 ul	2 ul	2 ul	2 ul
Template	1 ul	1 ul	1 ul	1 ul	1 ul

Temperature	Time	Cycles
98°C	30 sec	1X
98 °C	10 sec	35X
Tm	5 sec	
72 °C	5 sec	
72 °C	1 min	1X

Following extension PCR, 2% agarose gel electrophoresis is run to assess for successful amplification of insert fragments. Amplicons of desired lengths are observed.

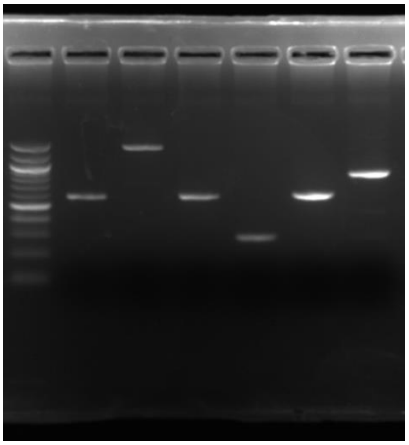

Figure 7 2% Agarose gel electrophoresis of inserts amplified by extension PCR. Lane 1, Quick-Load® 100 bp DNA Ladder. Lane 2, CMV. Lane 3, IRES-eGFP. Lane 4, U6-miR26a. Lane 5, CMV-NLVPMVATV. Lane 6, U6-miR26a-U6.

The fragments are added to PCR mix without primers to splice the 5 individual fragments of the insert. After the first round of PCR, primers that flank the entire insert sequence (CMV-SIINFEKL-U6-miR26a-U6) is added to the reaction amplify the entire insert containing all fragments.

First round of PCR without primers:

Reagent	Volume
ddH_2O	15 ul
2x Phanta Flash Master Mix	20 ul
CMV (56.5 ng/ul)	1 uL
SIINFEKL (6.9 ng/ul)	1 uL
IRES-eGFP (134.2 ng/ul)	1 uL
U6-miR26a (57.2 ng/ul)	1 uL
U6 (28.9 ng/ul)	1 uL

Temperature	Time	Cycles
98°C	30 sec	1X
98 °C	10 sec	35X
Average Tm of all homologous sequence	5 sec	
72 °C	5 sec	
72 °C	1 min	1X

Second round of PCR:

Reagent	Volume
Forward primer (10uM)	2 uL
Reverse primer (10uM)	2 uL
Product of first round PCR	40 uL

Temperature	Time	Cycles
98°C	30 sec	1X
98 °C	10 sec	35X
Tm	5 sec	
72 °C	5 sec	
72 °C	1 min	1X

1% agarose gel electrophoresis is run to verify the overlapping PCR result. A clear band at between 2500-3000bp is observed, indicating the successful recombination of the 5 fragments. Gel purification is then performed using kit from Qiagen.

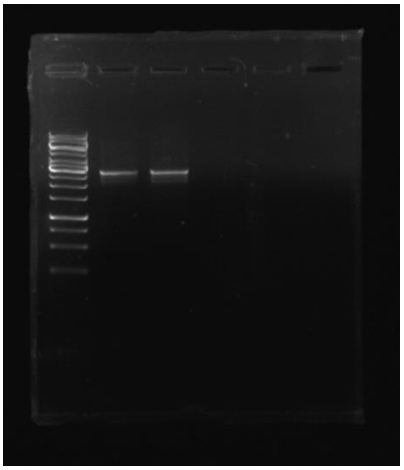

Figure 8 1% agarose gel electrophoresis of CMV-SIINFEKL-U6-miR26a-U6. Lane 1, GeneRuler 1kb DNA ladder. Lane 2-3, CMV-SIINFEKL-U6-miR26a-U6

Target plasmid pAAV-a2bMAFP-SIINFEKL-hTERT-miR26a-hTERT-miR28 from Genscript is used as backbone for cloning of the control plasmid. Restriction enzyme digestion is first performed with MfeI from New England Biolabs with the following master mix, which is incubated at 37°C for 1 hour.

Reagent	Volume
H2O	75 ul
MfeI	5 ul
rCutSmart™ Buffer	10 ul
Plasmid (1 ug/ul)	10 ul

A 1% agarose gel electrophoresis is performed to assess for lengths of the digested product. A single band at around 8000bp is seen indicating success of MfeI digestion. Gel extraction is then performed using Qiagen's kit to extract the digested product for second single digestion. Purified DNA are eluted in 30 uL.

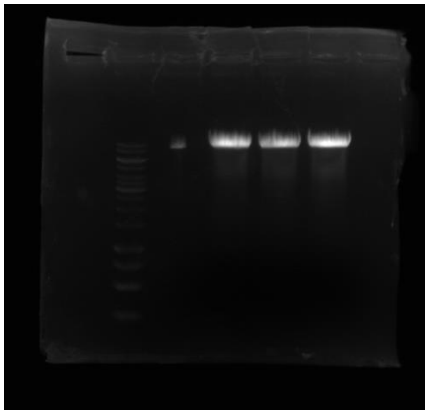

Figure 9 1% agarose gel electrophoresis of MfeI digested products. Lane 2, GeneRuler 1kb DNA ladder. Lane 2, 5uL MfeI digested products. Lane 3-6, remaining volume of MfeI digested products.

A second restriction enzyme digestion in performed with FastDigest HindIII from Thermo Scientific, using the following mastermix.

Reagent	**Volume**
H2O	36ul
FastDigest HindIII	7ul
FastDigest Buffer	7ul
DNA obtained from previous gel extraction	20ul

To assess for the length of digestions, 1% agarose gel electrophoresis is run and gel extraction is performed. Band at 5000bp are seen, implying successful HindIII digestion.

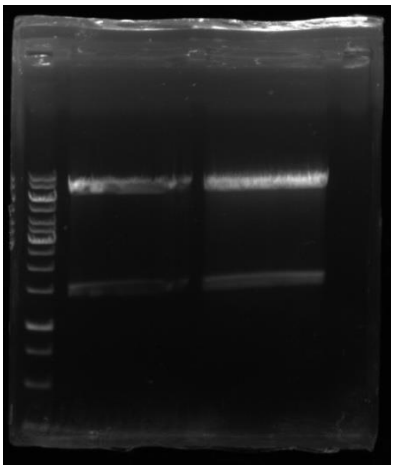

Figure 10 1% agarose gel electrophoresis of HindIII digested products. Lane 1, GeneRuler 1kb DNA ladder. Lane 2-3, HindIII digested products.

Recombination of the vector and insert is performed using ClonExpress II One Step Cloning kit from Vazyme. The linearized vectors and inserts are incubated with Exnase II at 37^{o}C for 30 mins. The resulting circularized plasmid is transformed into Stbl3 chemically competent *E coli.* cells by heat shock. Positive colonies are picked in grown in Ampicillin containing LB broth overnight. Maxiprep kit from Qiagen is used to extract the control plasmid from LB.

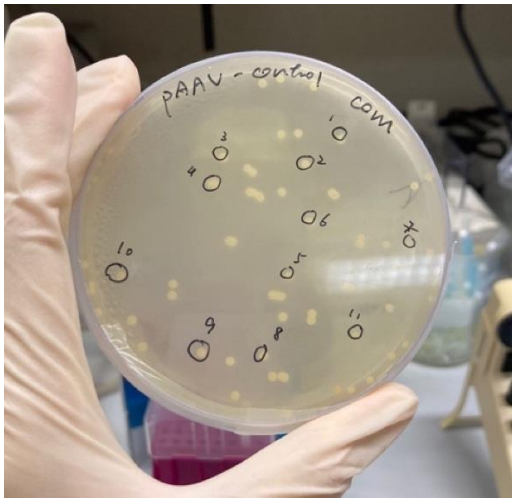

Figure 11 Bacterial colonies of transformed pAAV-CMV-SIINFEKL-U6-miR26a-U6-miR28

To perform colony PCR, the system is prepared as demonstrated below and incubated in 98°C for 10 minutes to lyse the bacteria.

Reagent	Volume
Phusion HF Buffer 5X	5 ul
H_2O	12 ul
dNTPs (10mM each)	1 ul
Forward primers (10uM)	1 ul
Reverse primers (10uM)	1 ul

Following the lysis of bacteria to release plasmid DNA, a mix 0.2 uL Phusion polymerase and 5 uL H_2O is added to each reaction. The program is then run as follow:

Temperature	Time	Cycles
94°C	2 min	1X
94 °C	30 sec	35X
Tm	30 sec	
72 °C	2.5 min	
72 °C	7 min	1X

1% agarose gel electrophoresis to assess for successful ligation of the insert onto the backbone. Both gel electrophoresis results and Sanger sequencing results from Tech Dragon Limited reveals successful cloning of the control plasmid.

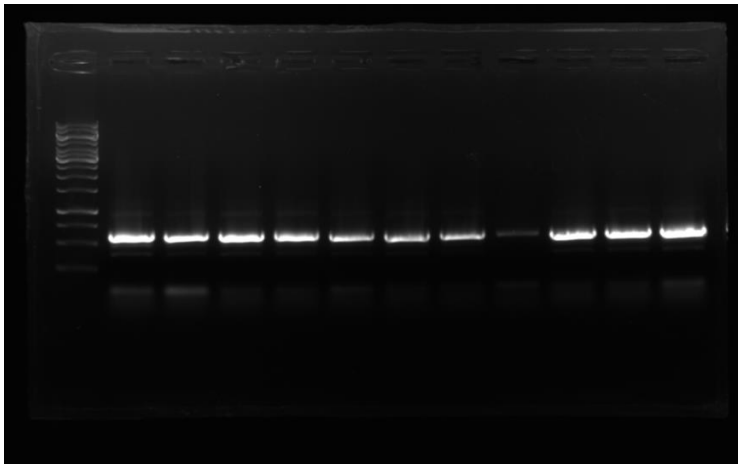

Figure 12 1% agarose gel electrophoresis of colony PCR products. Lane 1, GeneRuler 1kb DNA ladder. Lane 2-12, colony PCR products

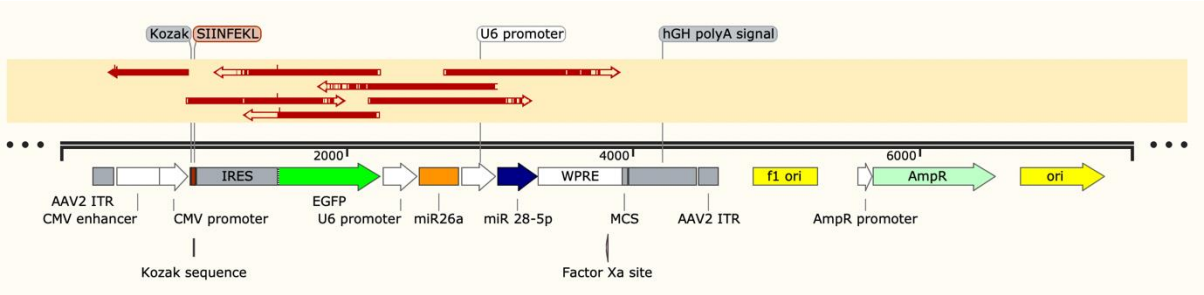

Figure 13 Sanger sequencing result of the pAAV-CMV-SIINFEKL-U6-miR26a-U6-miR28 after Maxiprep

c) Plasmid transfer into cell line

Transfection is performed using optimized ratio from part 2 of our engineering cycle. 293T, Huh7, and MIHA, are transfected by pAAV-CMV-SIINFEKL-U6-miR26a-U6-miR28 and pAAV-a2bMAFP-SIINFEKL-hTERT-miR26a-hTERT-miR28 using Lipofectamine 3000, at an ratio of 1:3, 1:4, and 1:6 respectively.

d) Immunostaining

72 hours after transfection, the transfected cells are fixed onto glass slides using formaldehyde. Blocking is performed by adding 3% 1X PBS. Fluorophore conjugated OVA257-264 (SIINFEKL) peptide bound to H-2Kb Monoclonal Antibody from eBioscience is diluted at a ratio of 1:20, and incubated at 4^{o}C overnight.

Test

To examine the transfection efficiency and expression of the SIINFEKL peptide, the three cell lines are examined under confocal microscope.

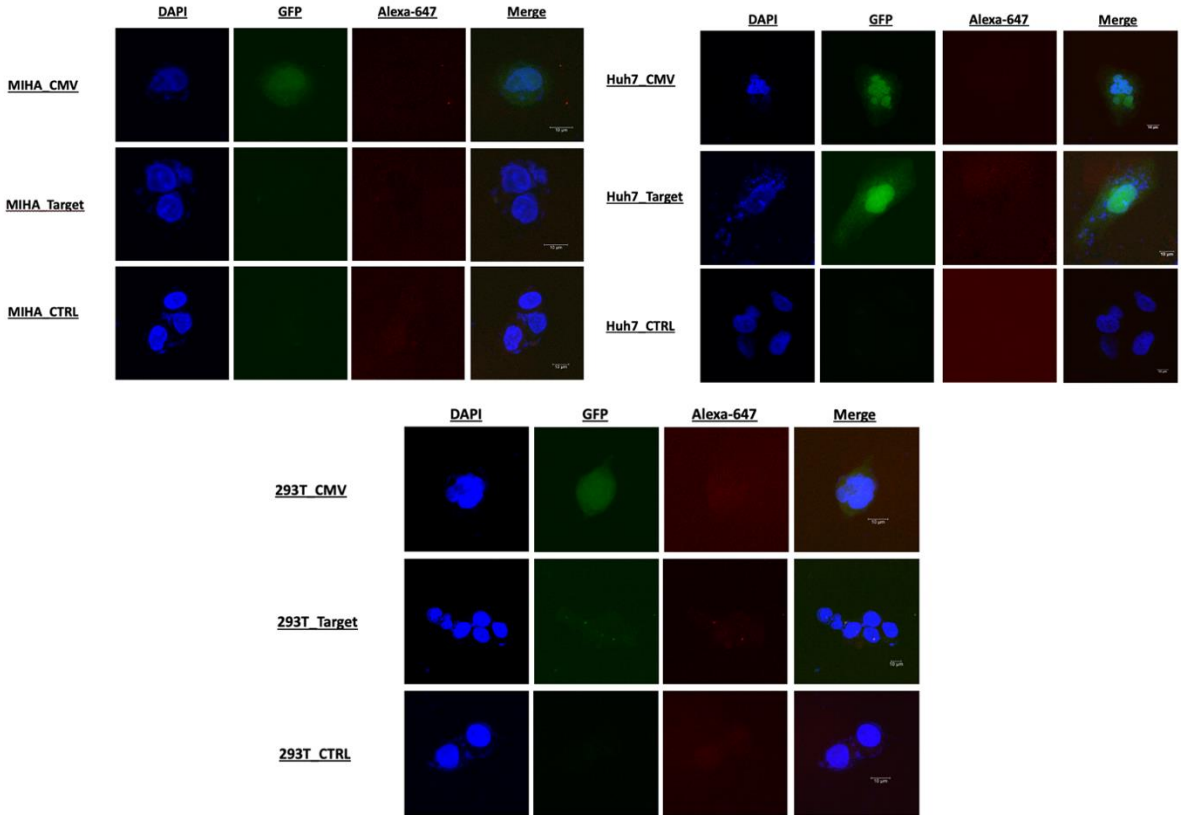

Figure 14 GFP and Alexa Fluor-647 expression, under a2bM-AFP promoters in MIHA, Huh7, 293T cells

Learn

We have successfully transfected all three cell lines, as evidenced from the presence of green fluorescence in MIHA, Huh7 and 293T cells transfected by the control plasmid (pAAV-CMV-SIINFEKL-hTERT-miR26a-hTERT-miR28). Specificity of the a2bM-AFP promoter is as well showcased by the presence of green fluorescent protein in target plasmid transfected HuH7 cells but not in MIHA and 293T cells.

It was to our surprise that the SIINFEKL peptide is not expressed and present to the surface in all the three cell lines. There are a few reasons that could lead to failure of expression of the antigenic epitope. Promoter activity and epigenetic regulations are problems on a genetic level. However, we have ruled out the possibility of a faulty promoter, since in cell lines transfected by both control or target plasmid, the SIINFEKL is unable to be expressed.

Another hindrance to transfection efficiency might be the length of insert sequence. As a long insert sequence severely hinders transfection as well as expression especially in bicistronic vectors, it might have played a role in the failure to express the antigen SIINFEKL. However, as GFP is expressed in all the cells lines transfected by control plasmid, hinting that insert length might not be the major factor contributing to the lack of SIINFEKL expression and loading onto the surface MHC.

Although GFP expression is observed in control cell lines, the expression level is rather low. After discussing with our instructor and advisors, a low transfection efficiency might be contributive to the low level of GFP expression. We have then decided to deliver our plasmids into cells by transduction instead of transfection. For the optimization of transduction, please refer to part 3.

We have also suspected the absence of SIINFEKL on MHC might be due to faulty vector design. This suspicion is confirmed after our meeting with Prof. Li (IHP), who has worked on AAV gene therapy for more than 20 years. SIINFEKL will only be expressed and loaded onto the MHC variant H-2Kb, which is only present in mice, but is not expressed in humans. Without the suitable MHC, red fluorescence could not be observed as the antibody could only bind to H-2Kb restricted SIINFEKL. It is of utmost importance for us to switch to an antigen that could be expressed on human MHC.

Part 2: Transfection optimization

Design

a) Transfection methods overview

For the transfection of AAV vectors, we plan to try out both cationic lipids (i.e., Lipofectamine 2000) and PEI since both are commonly used in past AAV studies.

Firstly, Lipofectamine 2000 mediates transfection by the neutralization of cationic lipids to negatively charged nucleic acids. The formation of an excessively positively charged DNA/lipid complex allows the complex to be uptaken by cells via endocytosis. It is chosen as one of the tested transfection methods because cationic lipid-mediated transfection generally results in a high transfection efficiency in most eukaryotic cells. In Gao's study (2018), the transfection with pHelper plasmid with Lipofectamine-mediated transfection resulted in a 10-fold higher expression than other transfection reagents such as SuperFect. From the results, it is concluded that lipid-based liposomes exerts least blocking effect on rAAV2 transfection. On top of the mentioned data, Lipofectamine 2000 is also chosen because prior to meeting with Prof. Li (IHP), we referenced his past publications, and Lipofectamine 2000 is often used to transfect 293T cells with AAV vectors. Therefore, we have decided also to test out the transfection efficiency with lipid-mediated transfection.

Another transfection method that we have often came across during our literature research is the polymer-based PEI method. PEI has the protonated nitrogen that is found in PEI molecules allow its ionic interactions with the phosphate backbone of DNA. The resultant polyplex will then be uptaken by cells. PEI is the most common transfection method used for AAV vectors because of its simple implementation, availability and low cost of raw materials. PEI is also found to be effective in both small- and large-scale AAV productions. In small-scale productions, past studies reported AAV2 and AAV5 vectors titers ranging from 0.3×10^{13} to 1.6×10^{13} VG/litre in suspension adapted HEK-293T cells can be achieved with PEI. While in large-scale production, the transfection efficiency also ranged from 54-99%, producing up to 10^{13} AAV vectors. In 3.5-litre bioreactor can even generate up to 10^{14} VG AAV2 vectors in suspension HEK-293T cells, and the efficiency of using PEI for AAV vector transfection in adherent 293T cells is also satisfactory.

Both methods will be tested in ratios ranging from 1:2 to 1:6 to decide the optimum concentration of transfection agents to be used.

b) Choice of cell line

We plan to use a total of 5 cell lines - Hep3B, Huh7, MIHA, 293T, and T-HESCS.

Hep3B and Huh7 are hepatocellular carcinoma cell lines. These two HCC cell lines are specifically chosen because they produce a high level of AFP (about 240 ng/mL and 50ng/mL respectively). Our chosen tumour-specific promoter - a2bm-AFP regulates gene expression according to the AFP level. According to Yoon (2020), the a2bm promoter demonstrated up to 2.8-fold higher luciferase activity in Huh7 cells. Therefore, both cell lines are expected to demonstrate the system's ability to target AFP-positive HCCs.

MIHA is a normal hepatocyte cell line. The inclusion of a normal hepatocyte cell line is to prove the specificity of our system, ensuring that the system would not render expression of the antigenic protein on healthy and normal liver cells. In normal hepatocytes, AFP and hTERT is not produced and thus elements driven by the tumor- and cancer-specific promoters should not be expressed.

293T and T-HESCS are kidney epithelial and endometrial fibroblast cell lines respectively. Both of these normal cell lines do not express AFP and are used as negative controls to test the system's specificity on AFP-positive cancerous cells.

c) Plasmid used for transfection optimization

The plasmid with CMV driven-green fluorescence protein (AAV-CMV-GFP) is constructed to visualize the transfection efficiency of AAV vectors in different cell lines using the two planned transfection methods. Since CMV is a constitutive promoter, it directs a high level of transient gene expression in most types of cells. The percentage of transfected cells will be estimated and measured according to the fluorescence level in GFP.

Build

a) AAV-CMV-GFP

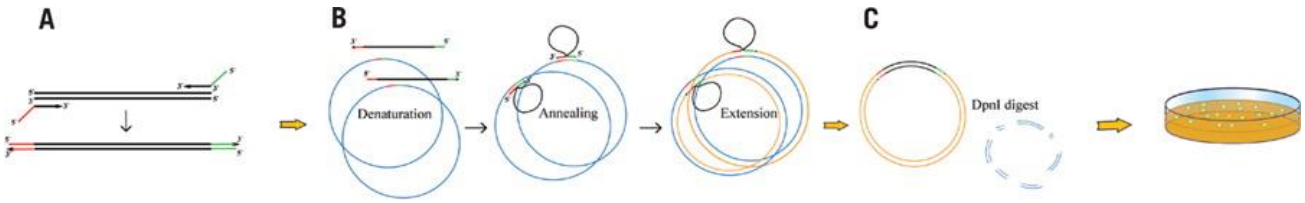

Figure 15 Overview of AAV-CMV-GFP cloning by overlap extension PCR

The rAAV2 backbone of transfer plasmid is obtained from Takara as the parental plasmid for overlapping extension PCR. GFP fragment are synthesized to contain 15 overlapping base pairs with the parental plasmid at both 5' and 3' ends of the fragment, flanking the site of insertion. The system and program used are as follow:

Reagent	Volume
ddH_2O	20 ul
2x Phanta Flash Master Mix	25 ul
Forward primer (10uM)	2 ul
Reverse primer (10uM)	2 ul
DNA template with GFP sequence	1 ul each

Temperature	Time	Cycles
98°C	30 sec	1X
98 °C	10 sec	35X
Tm	5 sec	
72 °C	5 sec	
72 °C	1 min	1X

After GFP fragment is extracted from gel using the Qiagen kit, agarose gel electrophoresis using 2% gel and 100bp ladder is performed to assess for successful generation of GFP fragment. Bright bands of desired length of approximately 700 bp is observed.

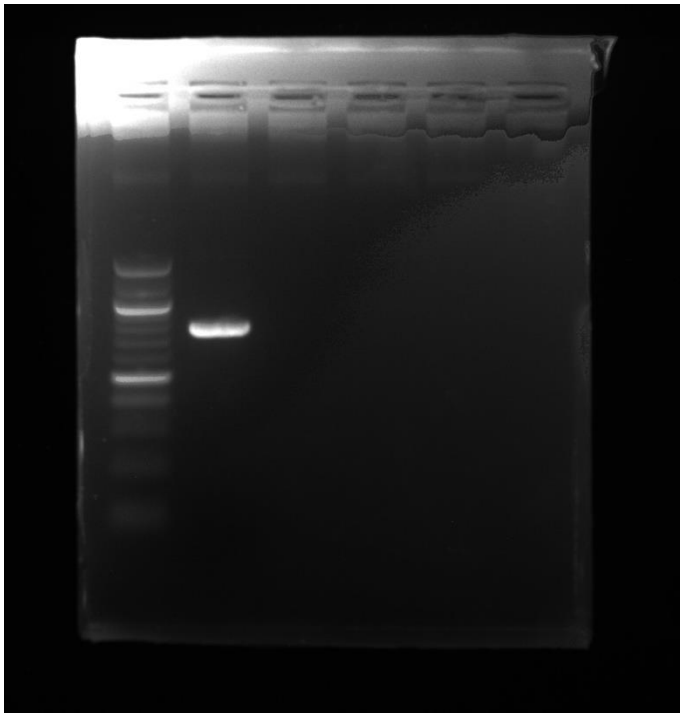

Figure 16 1% agarose gel electrophoresis of GFP fragment. Lane 1, Quick-Load® 100 bp DNA Ladder. Lane 2, GFP

After , GFP fragment is clone into the rAAV2 backbone using overlapping extension PCR using the following system and programme:

Reagent	Volume
ddH_2O	8 uL
2x Phanta Flash Master Mix	10 uL
GFP fragment (100ng/uL)	1 uL
Template (20 ng/ul)	1 uL

Temperature	Time	Cycles
98°C	30 sec	1X
98 °C	10 sec	35X
Tm	5 sec	
72 °C	45 sec	
72 °C	1 min	1X

The PCR product is immediately purified using gel extraction kit from Qiagen to remove salts for further procedures and eluted in 20uL ultrapure H_2O. Purified PCR products are digested overnight (~12 hrs) with DpnI at 37°C according to the following system:

Reagent	Volume
DpnI (Thermo Scientific)	2 uL
10X Buffer Tango	2 uL
Plasmid	16 ul

Utilizing the heat shock method, 10 uL of the DpnI digested product are transformed into100 uL Stbl3 chemically competent *E coli.* cells. Transformed competent cells are cultured on agar plate with ampicillin.

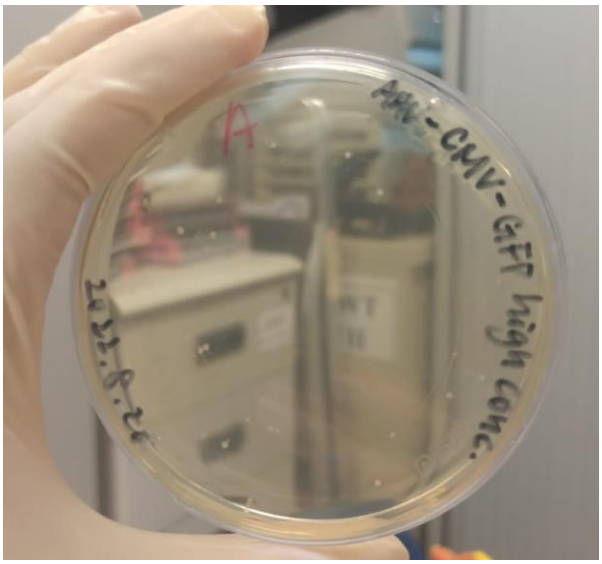

Figure 17 Bacterial colonies of transformed AAV-CMV-GFP

Bacterial colonies that grown on agar plate after overnight incubation at 37°C are selected for performing colony PCR. The system is demonstrated below and incubated in 98°C for 10 minutes to lyse the bacteria.

Reagent	Volume
Phusion HF Buffer 5X	5 ul
H_2O	12 ul
dNTPs (10mM each)	1 ul
Forward primers (10uM)	1 ul
Reverse primers (10uM)	1 ul

Following the lysis of bacteria to release plasmid DNA, a mix 0.2 ul Phusion polymerase and 5 ul H_2O is added to each reaction. The program is then run as follow:

Temperature	Time	Cycles
94°C	2 min	1X
94 °C	30 sec	35X
Tm	30 sec	
72 °C	2.5 min	
72 °C	7 min	1X

Gel electrophoresis with 2% agarose is conducted after the standard PCR. The band existence of around 700 bp provides partial evidence to the successful production of the plasmid with GFP insertion. Miniprep and maxiprep is then done to amplify the positive of colony PCR for Sanger sequencing and later experiments. Sequencing result from Tech Dragon Limited indicates the successful cloning of the AAV-CMV-GFP.

b) Transfection

We have performed transfection into 5 human normal or cancer cell lines (HuH7, Hep3B, HEK293T, MIHA, and T-HESCS) using Polyethylenimine, Linear, MW 25000 from Polysciences, and Lipofectamine™ 3000 Transfection Reagent from Invitrogen. As the ratio of DNA to transfection reagent is dependent on cell lines and AAV serotype, a range of ratio from 1:2 to 1:6 is applied to optimize the condition for transfection.

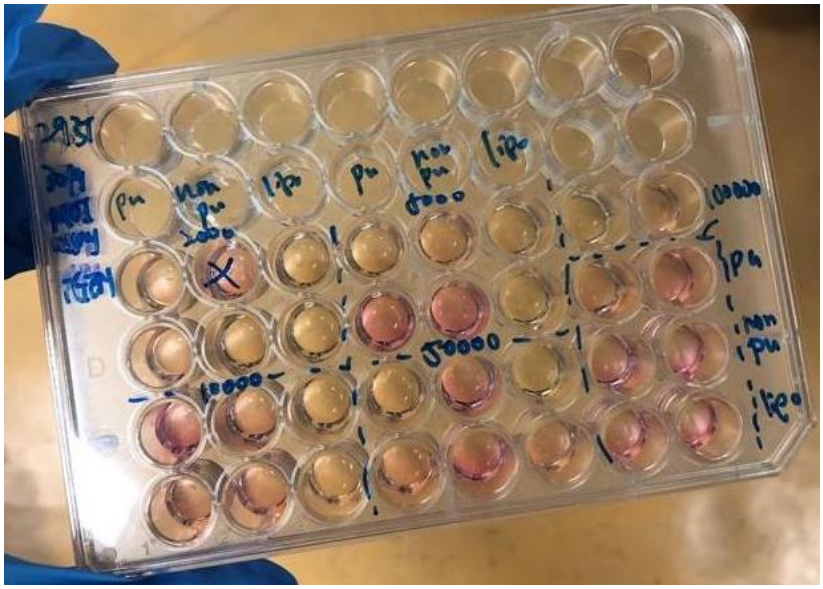

Figure 18 293T cell line transduced by AAV2-CMV-GFP obtained from different methods of co-transfection and purification at MOI ranging from 2000 to 50000

Test

We observed the GFP expression levels of various cell lines under fluorescent microscope. The photomicrographs could be accessed in the following document: https://docs.google.com/document/d/1hJOpLzQq6i4jFLRW7e46Hwc67Ys98pEZ/edit

Learn

The DNA:transfection reagent ratio is cell line dependent. For Huh7, cells transfected by pAAV-CMV-GFP using lipofectamine demonstrated a higher level of GFP expression than that of PEI at any ratio. However, since any ratio higher than 1:4 would cause significant cell death due to the cytotoxicity in Huh7, the optimal transfection condition for Huh7 would be a DNA:Lipofectamine 3000 ratio of 1:4.

For Hep3B, cells transfected by PEI generally have a higher level of expression than Lipofectamine 3000. The ratio of 1:5 is optimal as higher ratio might result in significant cell death due to the cytotoxicity of Lipofectamine 3000. However, the cell viability has decreased significantly in the following week. Hence, we have decided not to include this cell line in our prototype demonstration.

For T-HESCS and MIHA, the normal cell lines have a low level of GFP expression for transfection done by PEI and Lipofectamine3000. We have decided to use Lipofectamine

3000 at a ratio of 1:6 as its shows a slightly higher GFP level. After a week, the cell viability of T-HESCS greatly deteriorated. Hence, we have decided only to employ MIHA as our normal hepatocyte cell line.

For HEK293T cells, they have a high transfection efficiency in general. Both PEI and lipofectamine 3000 give a good transfection result for 293T. However, lipofectamine 3000 in the ratio of 1:3 to obtain is suggested due to both high transfection efficiency and high cell viability.

Cell line	**DNA:Lipofectamine 3000**
Huh7	1:4
HEK293T	1:3
MIHA	1:6

Part 3: Transduction optimization

Design

Since the result of transfection alone is not ideal and promising, we decided to switch the whole project design to AAV packaging. The decision is made by two main reasons: 1) transfection efficiency may not reflect virus packaging and transduction efficiency; 2) transfection result alone cannot fully model how our system works eventually. Some cell lines, especially the normal cell lines, are very hard to be transfected no matter how we optimise the condition for transfection, raising the difficulty of proving our concept. However, having low transfection efficiency doesn't mean that the infection rate is low as well. There is no known correlation between two. Besides, it is the viral vectors that will be delivered to the patients eventually but not the plasmid alone. Transfection result alone cannot completely simulate how our system interacts with different types of cells in the body and produces therapeutic effects. With these concerns, performing AAV packaging and transduction will be a better experimental design to prove our concept.

AAV packaging and transduction are optimised in several aspects: 1) choice of transfection reagent; 2) extraction and purification methods; 3) multiplicity of infection (MOI).

a) Choice of transfection reagent

Lipofectamine™ 2000 from Invitrogen and Polyethylenimine, Linear, MW 25000 (PEI) from Polysciences were used for transfection to evaluate which one is a better transfection reagent in terms of cell viability and transfection efficiency.

b) Extraction and purification method

2 different sets of extraction and purification methods are tried out: commercial AAV purification kit from Takara and iodixanol gradient centrifugation. The former one includes a column for purification in which AAV viral particles will bind onto resin in the column until the elution step. No centrifugation is required, unlike the iodixanol gradient centrifugation. Desalting and concentration of AAV were done by flowing the eluted virus through the filter device provided in the kit. For the iodixanol gradient centrifugation, we extracted AAV from cells by freeze-thaw method while purified AAV using iodixanol (OptiPrep) gradient ultracentrifugation. Real-time PCR (qPCR) is performed to measure the virus titre after purification of AAV to evaluate which method has a greater performance.

c) Multiplicity of infection

MOI is dependent on the choice of viral vector and cell lines. Optimising the MOI is extremely important to maximise the transduction efficiency. Low MOI causes low infection rate while high MOI may result in cytotoxicity. To find a balance between two, a MOI assay is performed in each cell line to test for the optimal MOI. MOI that produces greatest transduction efficiency while minimal cytotoxic effect will be chosen for our later part of the experiment.

Build

To produce a high yield of AAV, 10^7 HEK293T cells were plated on one 15 cm culture dish and a total of 20 culture dishes were used for packaging.

4 set-up, each set-up accounts for 5 dishes
1. Lipofectamine™ 2000; AAVpro® Purification Kit (AAV2) from Takara
2. Lipofectamine™ 2000; Iodixanol gradient centrifugation
3. PEI; AAVpro® Purification Kit (AAV2) from Takara
4. PEI; Iodixanol gradient centrifugation

pAAV-CMV-GFP, pRC2-mir342 and pHelper in AAVpro® Helper Free System (AAV2) from Takara were co-transfected into HEK293T cell and two different transfection reagents were used for optimization. They are PEI and Lipofectamine™ 2000. The ratios of transfection reagent to plasmid are as follows:

	Transfection reagent	plasmid	Ratio (plasmid : transfection reagent)
Lipofectamine™ 2000	90µl	10µg for each plasmid; Total of 30µg were used	1:3
PEI	240µl	26µg of pHelper; 17µg of pRC2-mir342; 17µg of pAAV-CMV-GFP; Total of 60µg were used	1:4

72 hours after co-transfection, extraction and purification of AAV were done to yield the viral particles. As aforementioned, two sets of methods were used for extraction and purification. For iodixanol gradient centrifugation, a total of four layers of iodixanol gradients are overlaid in a Ti45 centrifugation tube, from bottom to top: 60%, 40%, 25%, 17%. AAV supernatant is added to the top centrifuged at 40000rpm for 3 hours. The 40% layer was collected then purified using Amicon 100K columns from Merck Millipore.

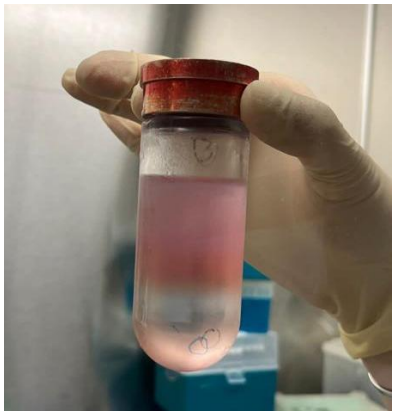

Figure 19 Iodixanol gradient in ultracentrifuge tube. The four layers are 60%, 40%, 25%, 17% from bottom to top.

For AAVpro® Purification Kit (AAV2), we followed manufacturer's protocol to extract, wash, elute, desalt, and concentrate the AAV2.

Figure 20 Lysed HEK293T cells passing through resin column, using AAVpro® Purification Kit(AAV2).

To quantify the amount of genome-containing AAV-CMV-GFP, AAV titration using SYBR Green technology is performed. qPCR is done to measure the number of inverted terminal repeats (ITRs) of AAV2, which gives an estimation of AAV2 present in the extracted solution. An pAAV-CMV plasmid of known concentration was used as standard.

Next, from the virus we obtained, we tried to transduce the cell lines with different multiplicity of infection (MOI), ranging from 2000 to 150000. We only used virus that produced from commercial kit and packaged with Lipogfectamine^{TM}2000 to perform MOI test as it has the highest virus titre.

Cell line	MOI tested
HEK293T, Huh7	2000, 5000, 10000, 50000, 100000
MIHA	10000, 50000, 100000, 150000

Test

a) Packaging result

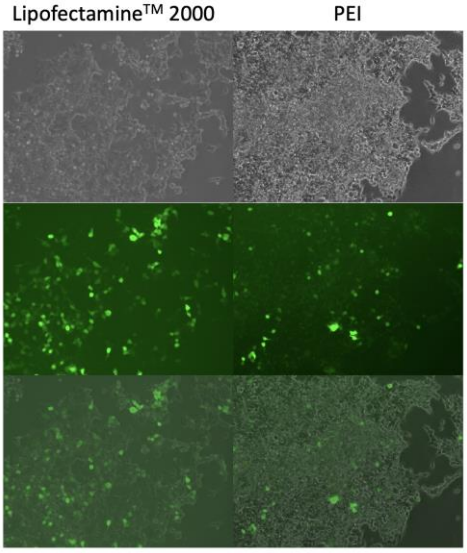

Figure 16 AAV packaging in 293T

From the above photos, Lipofectamine™ 2000 has a better transfection efficiency than PEI with high cell viability. We decided to use Lipofectamine™ 2000 as the transfection reagent for our real experiment.

b) AAV titration result

Standard curve of AAV is constructed after obtaining the result of AAV titration. Virus titre is then calculated.

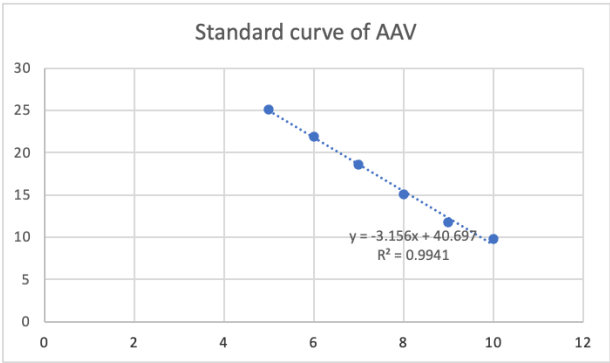

Figure 21 Standard curve obtained from AAV titration

Transfection reagent; extraction and purification methods	AAV titre	Amount of AAV
Lipofectamine™ 2000; Commercial kit	244473827.8	4.9E+10
Lipofectamine™ 2000; Iodixanol gradient centrifugation	188912244.4	3.8E+10
PEI; Commercial kit	62404624.13	1.2E+10
PEI; Iodixanol gradient centrifugation	244473827.8	3.9E+09

In general, using commercial kit produces a higher yield of AAV than freeze-thaw and ultracentrifugation methods. Freeze-thaw and ultracentrifugation methods are time-consuming and requires skilful techniques in order to prevent loss of virus and inclusion of impurities. Any careless handling may lead to low AAV titre. Using commercial kit is a much easier and more efficient way to yield high AAV titre.

c) MOI test result

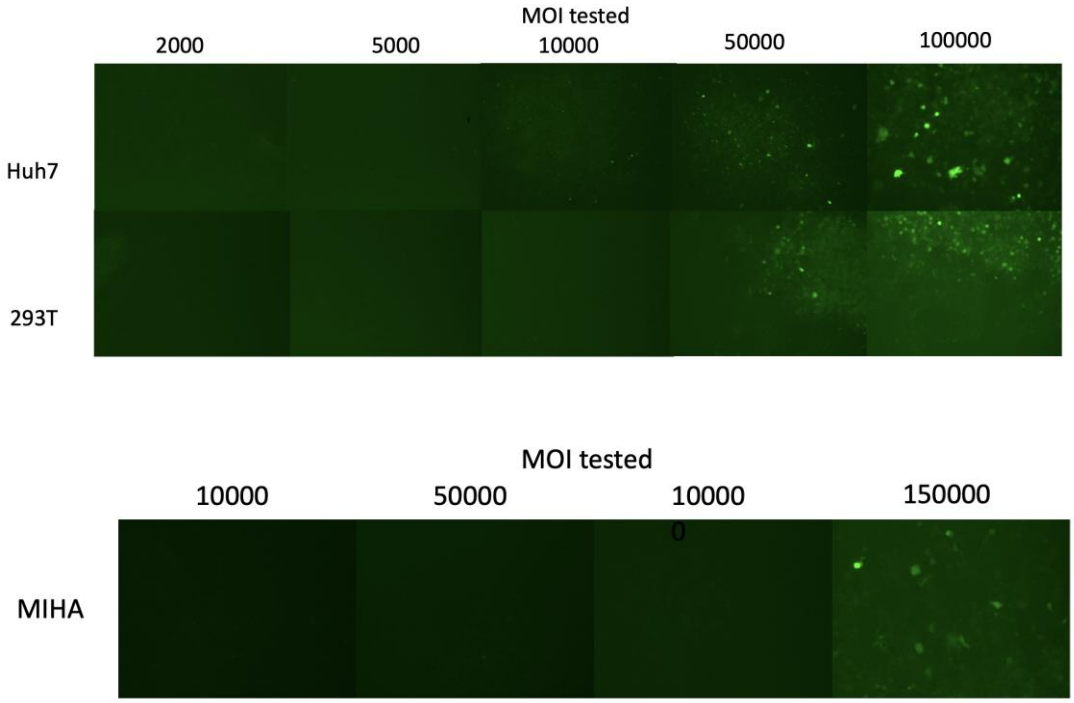

Figure 17 MOI test result of HUH7, 293T and MIHA

Based on the results above, we determined the MOI for different cell lines:

Cell line	MOI determined
Huh7, 293T	100000
MIHA	150000

Learn

As aforementioned, low cell viability was a great problem we encountered when doing transfection only on different cell lines. However this problem was not observed when packaging cell lines in HEK293T. Conditions for packaging and in vitro transduction were optimised and we decided to perform these with our control and target plasmids.

Part 4: Final plasmid construction and testing

Design

a) Antigenic peptide - NLVPMVATV

From Part 1, we have learnt SIINFEKL will not be expressed and loaded onto human MHC-1 complex. We turned to an immunogenic viral peptide from the cymegalovirus (CMV). CMV 65kDa phosphoprotein (pp65) antigen derived nonamer NLVPMVATV (residues 495-503) is predominantly displayed on HLA-A*02:01, which is the most abundant MHC-I variant in human population. CMV pp65 is selected for its non-human origin, thereby reducing the on-target off-tumour effects caused by conventional CAR-T therapy, which targeted antigens that could be found in both healthy and tumor cells. In addition, CMV pp65 is able to evoke cytotoxic T lymphocyte (CTL) response, with the NLVPMVATV as the most immunogenic epitope. CMV is asymptomatic in healthy individuals, while its seroprevalence is around 70% in industrialized countries and up to 100% in emerging countries. Infected subjects have shown high frequencies of HCMV-CTL positivity, with 70-90% of them specifically recognizing pp65 protein. Isolated from the 65kDa-protein, residue 495-503 could be used to amplify a memory CTL response. 40% of NLVPMVATV sensitized fibroblast was lysed by CTL from HCMV seropositive individuals in vitro.

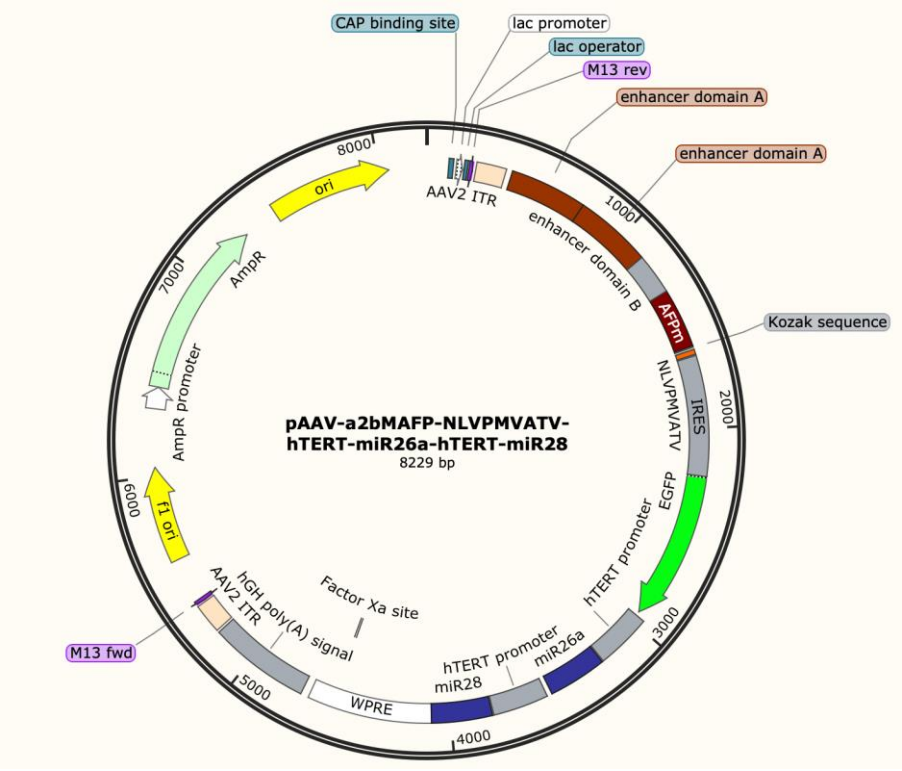

Figure 22 Plasmid map of pAAV-a2bMAFP-NLVPMVATV-hTERT-miR26a-hTERT-miR28

Build

a) Target plasmid (pAAV-a2bMAFP-NLVPMVATV-hTERT-miR26a-hTERT-miR28) construction

Site-directed mutagenesis is performed to replace Kozak-SIINFEKL from target plasmid and control plasmid with Kozak-NLVPMVATV. Primers are specially designed using SnapGene software according to Figure 2. to conduct such large substitution into the parental plasmids. To be concise, each equal halves of NLVPMVATV sequence are incorporated into the 5′ ends of both primers. 5′-overlapping regions of 8 nt are also designed for two primers. Each primer has 16 nt that are complementary to the template at the 3’ ends.

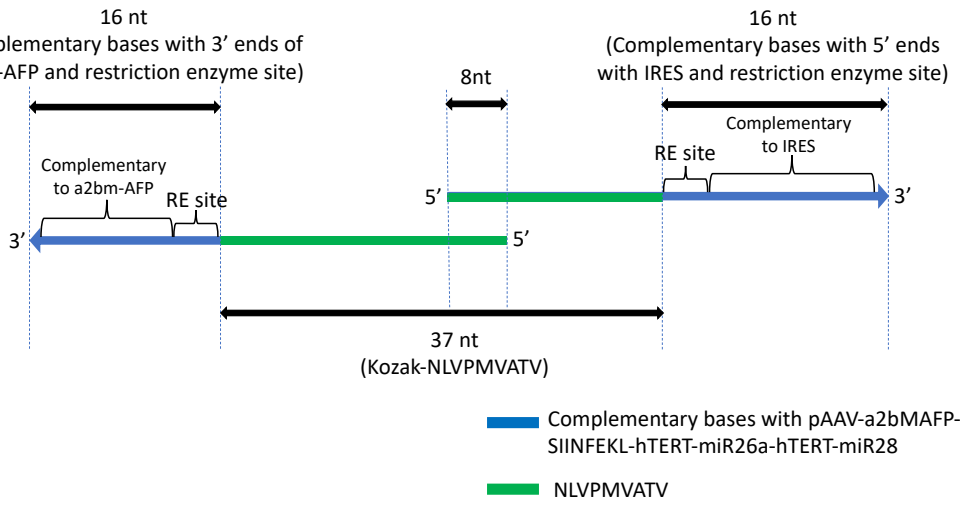

Figure 23 Primer design to construct pAAV-a2bMAFP-NLVPMVATV-hTERT-miR26a-hTERT-miR28 by site-directed mutagenesis

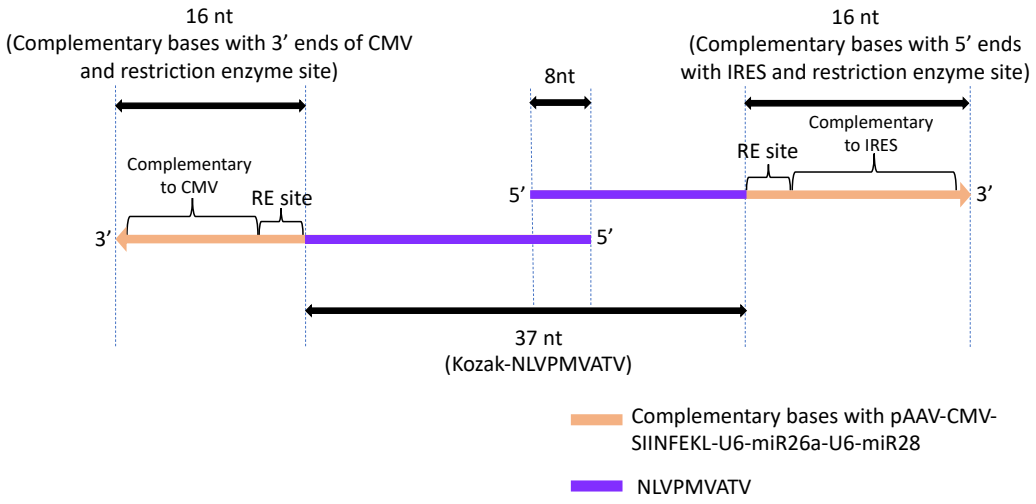

Figure 24 Primer design to construct pAAV-CMV-SIINFEKL-U6-miR26a-U6-miR28 by site-directed mutagenesis

Standard polymerase chain reaction (PCR) of 35 cycles is performed to synthesize the mutated fragment with the insertion of Kozak-NLVPMVATV using the two parental plasmid. The system and program used are as follow:

Reagent	Volume
ddH_2O	20 ul
2x Phanta Flash Master Mix	25 ul
Forward primer (10uM)	2 ul
Reverse primer (10uM)	2 ul
Template (pAAV-a2bMAFP-NLVPMVATV-hTERT-miR26a-hTERT-miR28/ pAAV-CMV-SIINFEKL-U6-miR26a-U6-miR28) (20 ng/ul)	1 ul

Temperature	Time	Cycles
98°C	30 sec	1X
98 °C	10 sec	35X
Tm	5 sec	
72 °C	45 sec	
72 °C	1 min	1X

Gel electrophoresis of the PCR product is then conducted using 1% agarose gel to identify the correct band of the DNA fragment with Kozak-NLVPMVATV substitution, which is approximately 8000 bp. Due to low concentration of newly synthesized DNA in previous trials, the DNA generated using pAAV-CMV-SIINFEKL-U6-miR26a-U6-miR28 as template undergoes PCR purification directly without performing gel electrophoresis.

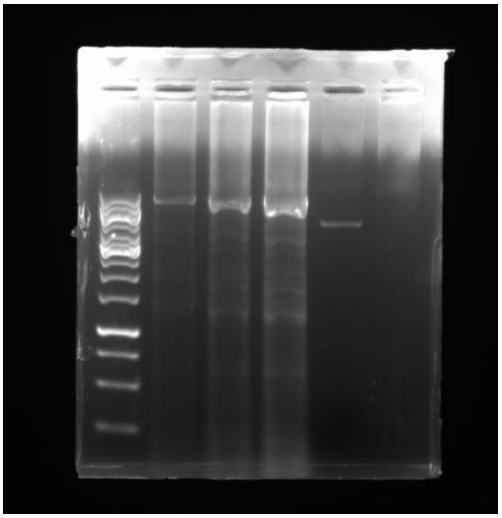

Figure 25 1% agarose gel electrophoresis of PCR product after site directed mutagenesis using pAAV-a2bMAFP-NLVPMVATV-hTERT-miR26a-hTERT-miR28 as template. Lane 1, GeneRuler 1kb DNA ladder. Lane 2, 1 uL PCR product. Lane 3, 5 uL PCR product. Lane 4, 10 uL

After the two DNA fragments with Kozak-NLVPMVATV insertion undergo extraction purification using kit from Qiagen and eluted in 30 ul ultrapure H_2O, they are digested with DpnI enzyme overnight to cleave the template plasmid of PCR. The system and program used are as follows:

Reagent	Volume
DpnI (Thermo Scientific)	2 ul
10X Buffer Tango	3 ul
DNA to be digested	25 ul

10 uL of DpnI digested product is transformer into Stbl3 chemically competent *E coli* by heat shock method. Bacteria are allowed to grow into colonies on agar plates with ampicillin after overnight incubation. Miniprep is performed later to amplify plasmid for restriction enzyme digestion. Plasmids are digested by restriction enzyme for 1 hr for 37^{o}C using the following system and program to verify the successful construction of mutated plasmid by observing the gel band size:

Reagent	Volume
H_2O	20.5 ul
XbaI	0.5 ul
NdeI	0.5 ul
rCutSmart™ Buffer	2.5 ul
Plasmid (500 ng/uL)	1 ul

Reagent	Volume
H_2O	20.5 ul
XbaI	0.5 ul
ApaI	0.5 ul
rCutSmart™ Buffer	2.5 ul
Plasmid (500 ng/uL)	1 ul

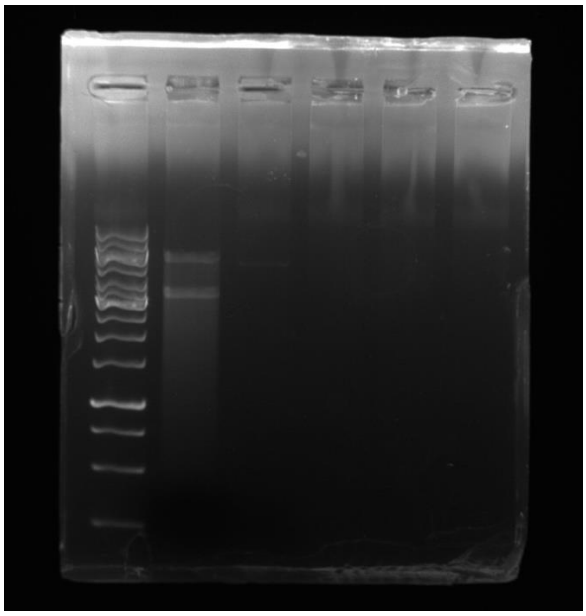

Figure 26 1% agarose gel electrophoresis after restriction digestion of pAAV-a2bMAFP-NLVPMVATV-hTERT-miR26a-hTERT-miR28 for verification. Lane 1, GeneRuler 1kb DNA ladder. Lane 2, restriction digested product, bright bands around 6000 bp and 3500 bp. Lane 3, undigested pAAV-a2bMAFP-NLVPMVATV-hTERT-miR26a-hTERT-miR28 as control.

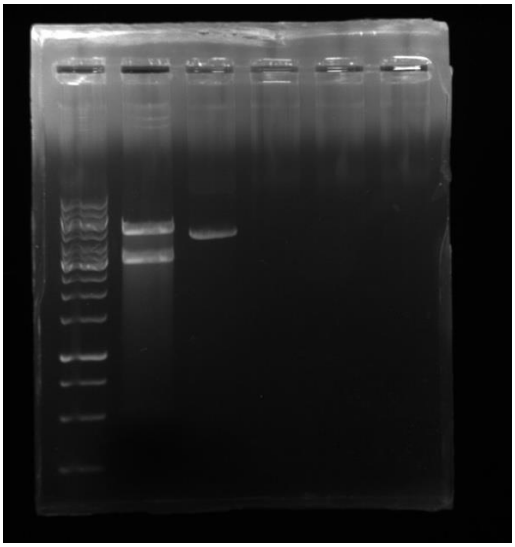

Figure 27 1% agarose gel electrophoresis after restriction digestion of pAAV-CMV-NLVPMVATV-U6-miR26a-U6-miR28 for verification. Lane 1, GeneRuler 1kb DNA ladder. Lane 2, restriction digested product, bright band around 5000 bp and 3000 bp . Lane 3, pAAV-CMV-NLVPMVATV-U6-miR26a-U6-miR28 as control

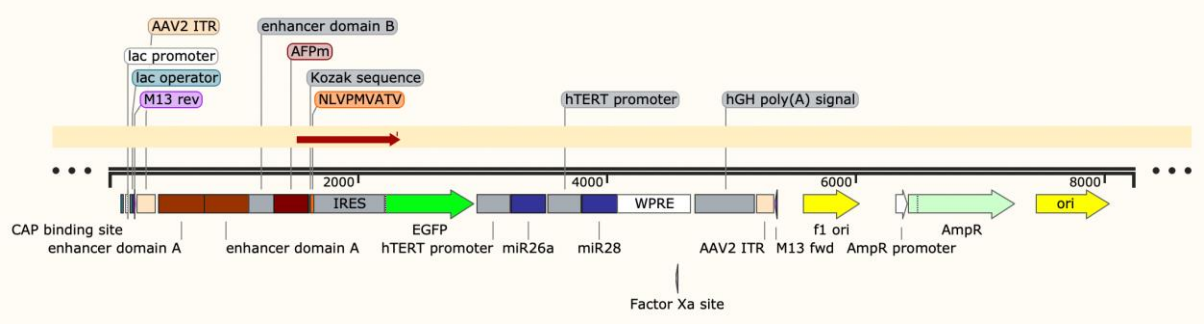

Figure 28 Sanger sequencing result of pAAV-a2bMAFP-NLVPMVATV-hTERT-miR26a-hTERT-miR28

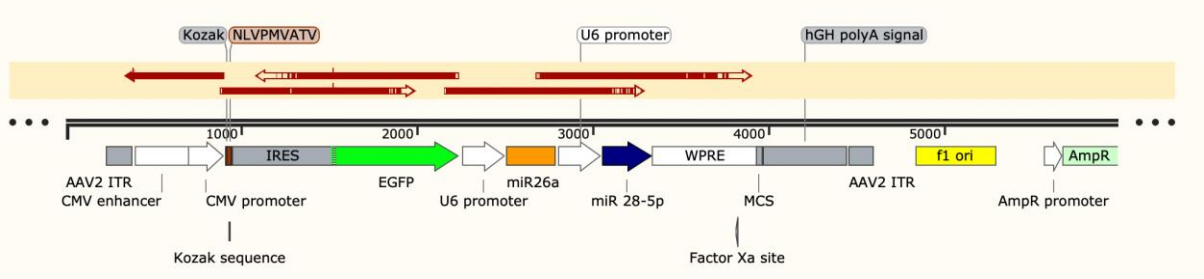

Figure 29 Sanger sequencing result of pAAV-CMV-NLVPMVATV-U6-miR26a-U6-miR28

b) Transduction

Transduction is performed using optimized condition from part 3. Co-transfection of pAAV-a2bMAFP-NLVPMVATV-hTERT-miR26a-hTERT-miR28 or pAAV-CMV-NLVPMVATV-U6-miR26a-U6-miR28, pRC-miR342, and pHelper is performed on HEK293T cells using Lipofectamine 2000. 3 days after co-transfection, the HEK293T cells were collected. AAV were extracted and purified using AAVpro® Purification Kit(AAV2) from Takara.

AAV titration is performed by qPCR using SYBR™ Green PCR Master Mix from Applied Biosystems. Huh7, MIHA, and HEK293T are infected with a MOI of 100 000, 150 000, and 100 000 respectively.

Test

To quantify expression levels of GFP and the CMV pp65 antigen NLVPMVATV, flow cytometry is performed (Fig. 30). CMV pp65 nonamer NLVPMVATV was determined by using Alexa Fluor™ 647 (Invitrogen, #A20186) labelled Anti-CMV (pp65-495) (NLVPMVATV) TCR-Like Antibody (H9), HLA-A*0201-Restricted (Creative Biolabs, #TCR-LA-ZP136). Data was analyzed with FlowJo software (v10, TreeStar).

The untreated groups are analysed to obtain background levels of GFP and NLVPMVATV. The GFP and NLVPMVATV positive cells are obtained by the percentage population of positive cells in the gated region minus the corresponding population in the untransduced cells.

		CMV+ %	GFP+ %
Huh7	Control plasmid	13.6	52.32
	Target plasmid	14.5	15.02
MIHA	Control plasmid	1.21	7.69
	Target plasmid	3.28	-1.13
293T	Control plasmid	4.33	8.93
	Target plasmid	6.95	3.07

The AFP-positive Huh7 has the highest level of NLVPMVATV expression driven by the tumor-specific promoter a2bM-AFP among the three cell lines. However, since the transduction efficiency is higher in Huh7 than MIHA and 293T, the higher level of NLVPMVATV present might be due to higher transduction efficiency rather than promoter specificity.

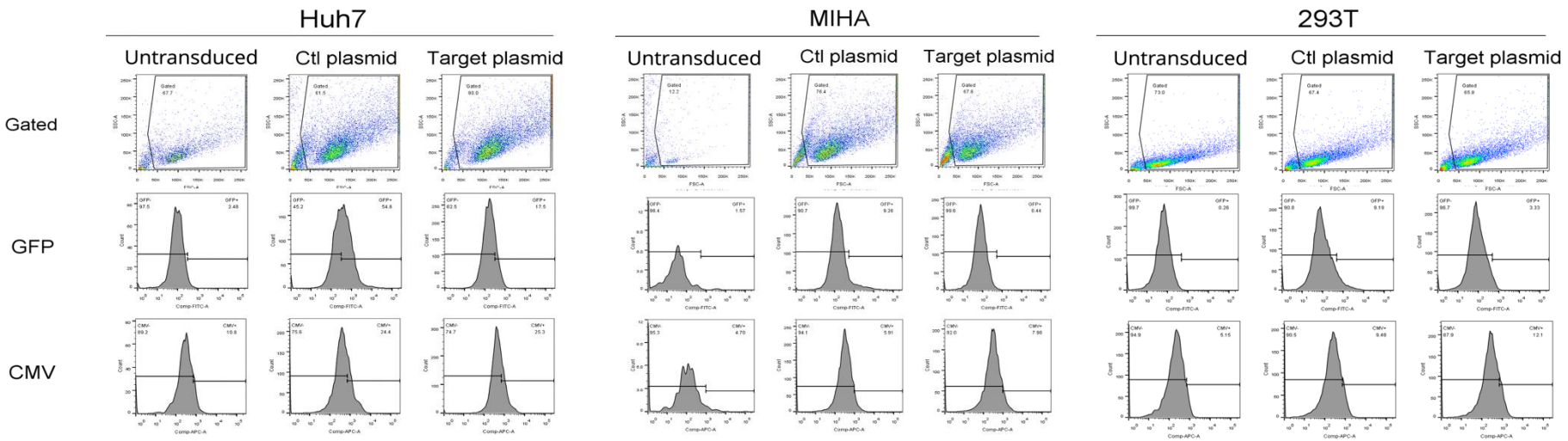

Figure 30 Fluorescence-activated cell sorting (FACS) plots of Huh7, MIHA and 293T cells, untransduced, transduced with control plasmid, or transduced with target plasmid after 72 hours of AAV infection. Percentage indicates GFP or NLVPMVATV positive cells in the gated region.

Learn

The results obtained from flow cytometry is not representative enough to conclude the tumor-specificity of the a2bM-AFP promoter, as Huh7 generally have a higher AAV transduction efficiency than 293T and MIHA. Whether did the enhanced transduction efficiency or the promoter-specificity, or both, played a role in improving NLVPMVATV presentation is yet to be determined. Further studies are required to determine the specificity to ensure the safety of our system.

With the highest at 52.32% of GFP positive population, the transduction efficiency is still rather low. Further studies could be conducted with the aim to enhance the transduction efficiency, primarily by shortening the insert sequence.

As the antibodies we used are HLA*02:01 restricted, it will only measure the HLA*02:01 restricted NLVPMVATV, but not the unbound NLVPMVATV, NLVPMVATV loaded on other HLA variants, or HLA*02:01 loaded with other peptides. Unlike the antibody, CAR T cells can bypass the MHC restriction and recognize the peptide as long as it is expressed on the surface of the tumor cells. When performed in vitro, the NLVPMVATV amount that could cause CAR T binding will always be underestimated, which suggests the significance of performing studies in vivo.

Of course, it would be the best if the NLVPMVATV could be loaded onto HLA Class I. We chose this immunogenic viral peptide for its ability to stimulate both cytotoxic T lymphocyte response as well as CAR T cell tumouricidal effects. While CAR T cells can bypass MHC restriction, cytotoxic T cells could only bind to epitopes presented by the HLA Class I. Hence, another direction would be to better understand the antigen expression and HLA loading pathway of NLVPMVATV, so that some minigenes that can enhance NLVPMVATV loading onto HLA could be identified or developed.

Future direction

In the future, we would move on to further verify and polish the effectiveness of our therapeutic model.

Vector design optimization

AAV transduce optimally with an insert sequence of around 4.7kb between the two ITRs. For our current design, the insert length is 4784bp. The long insert length might have contributed party to a reduced transduction efficiency. Shortening of our insert length might be beneficial to further enhancing our transduction efficiency. Instead of IRES, we have planned to use porcine teschovirus-1 2A peptide (P2A) as internal ribosome skipping sequence. A 2A peptide has 19-22 bp and is first discovered between two proteins in members of the picornavirus family. A highly conservative sequence – GDVEXNPGP is shared by different 2As. 2A oligopeptides can mediate the cleavage of polypeptides during translation in eukaryotic cells. By ribosome skipping the synthesis of glycyl-prolyl peptide bond at the C-terminus of 2A peptide, two cleaved proteins are resulted without additional factors such as protease: the protein upstream of the 2A attaching to complete 2A peptide except for the C-terminal proline, and the protein downstream of 2A linked to one proline at the N-terminus. This 2A reaction is termed “Stop-Go” or “stop-carry on.” A multi-gene system based on 2A has multiple advantages: Firstly, multiple proteins can be expressed in equivocal amounts under the control of a single promoter. This helps to overcome a problem associated with other co-expression strategies, such as IRES, in which translation efficiency of the gene located before and after can be different. Secondly, with the small size of 2A protein, multiple proteins are cleaved with the minimized possibility of function loss. Lastly, proteins connected by 2A are always co-expressed because it is only dependent on the activity of ribosome, which is highly structurally conserved in eukaryotes. Out of four widely used 2A peptide variants (P2A, T2A, E2A, and F2A), P2A is shown to confer the highest cleavage efficiency (close to 100%) in both human cell lines and mouse liver. Hence, P2A is chosen to be inserted between each of the functional domains to enable clean cleavage and stoichiometric expression of our antigenic peptide NLVPMVATV and eGFP.

We could also explore the possibility of using another tumor-specific promoter of higher activity. Dr. Tang (IHP) have suggested us hTERT-CMV (hTC or TMC) fusion promoter. The TMC promoter combines a fragment of hTERT promoter, which is from bases -456 to -2 upstream of the start codon, and a minimized fragment of CMV promoter, which is of bases -1017 to -901 upstream of the human CMV major immediate early protein start codon. The promoter was first described in an oncolytic virotherapy that inserts the promoter in front of a GFP signal and E1A gene which is necessary for transcription of various proteins in adenoviral replication and thus leading to cell death. It is shown that the efficiency between a CMV promoter and a TMC promoter is comparable such that only the adenovirus with CMV or TMC promoter undergoes effective viral replication and gives visible GFP light in cancer cell lines (fresh DLD-1 cells). In terms of cancer specificity of TMC promoter, the E1A expression was only detected in lung cancer cell line H1299, pancreatic cancer cell line MiaPaca-2 and colon cancer cell line DLD-1, but not in infected normal cell line NHFBs in the experiment. The promoters in the same plasmid design have also been tested in tumor-bearing mice whereas the results show that the viral transgene expression and replication

were efficient in tumour, proven by detectable GFP signals in the tumor. The promoter was further proven in another literature as a promoter for delivering truncated CD19 to cancer surface as a tumor tag. It is shown that while compared to hTERT and Survivin-driven promoters, the truncated CD19 were even better expressed by using TMC promoters.

AAV pseudotyping

During our literature research and meeting with Dr. Chow, it has come to our attention that pre-existing immunity to AAV could be a major obstacle to our system. AAVs are relatively common in the environment and its seroprevalence is up to 90% in human populations, easily resulting in capsid-mediated humoral immunity. Out of all AAV serotypes, the highest neutralizing factor seroprevalences detected are for AAV1 (50.5%) and AAV2 (59%), while the lowest is observed in AAV8 (19%) and AAV5 (3.2%). In order to improve the efficacy of our system, we think a feasible way would be to adopt AAV pseudotyping. Pseudotyping is the process of producing viruses in combination with a foreign viral envelope protein, thus circumventing the pre-existing immunity to highly prevalent serotypes. AAV pseudotyping is not an unprecedented practice, in fact it has been used in various studies to improve tropism and transduction efficiencies. Since AAV2 is the most well characterized vector in gene therapy, the efficacy of hybrid plasmids created by packaging AAV2 in capsids from different AAV serotypes (namely AAV2/1-8) are well studied. For example, it is known that AAV2/1 and 2/7 vectors transduce particularly well in muscles, while AAV2/8 is effective in liver-directed gene delivery.

In the future, a possible way to improve our system is by building a AAV2/5 pseudotype. This is because AAV5 is the least prevalent AAV serotype, meaning that immune responses are less likely to be triggered when the patient is being injected with AAV coated in AAV5 capsids. This will help to extend the application of our system to larger proportion of the general public. Moreover, Meumann's mechanistic study shows that the intracellular conditions in HCC promotes the release of vector genomes from the AAV capsid, this shows that AAV2's natural tropism to HCC is mainly mediated by the enhanced intracellular processing in HCC's microenvironment but not its capsid. Therefore, pseudotyping would be a perfect way to avoid pre-existing immunity whilst having low risk of compromising AAV2's existing tropism for HCC.

In vivo testing

We have used promoter-positive and control cell lines are used to evaluate the expression of therapeutic genes and their effects at the molecular level. Despite the usefulness of cancer cell lines as a simulation of actual human tumors, they lack the ability to mimic *in vivo* tumor microenvironment, which is particularly important as one of the goals of our therapeutic design is to facilitate immune cell infiltration. Besides, AAV has a low efficiency in *in vitro* experiments. Therefore, our next step would be implementing *in vivo* experiments in murine models to fill in the gaps of *in vitro* studies and study the efficacy of our AAV-CAR-T cell combined therapy as a complete treatment. Currently, common cancer mouse models used in preclinical studies include syngeneic tumor model, genetically engineered mouse model, and human xenograft model. Among them, the human xenograft model is commonly adopted in CAR T therapies and can best reproduce

the complicated conditions of human cancer. This type of model is prepared by injecting human cancer cell lines into immunocompromised mice and establishing an immune system through immune reconstruction or human immune cell transferring (Olson et. al, 2018). Taking the future prospective of our project and the need for a high analogy of the human tumor microenvironment into consideration, the human xenograft model would be our primary platform for experiments.

AAV delivery

Once mouse models are prepared, engineered AAV would be delivered. AAV is shown to be a safe and high-efficiency gene delivery vector and has been administered in over 2,000 clinical trials. Liver-directed AAV transfer could be implemented in several direct and indirect methods, including liver lobe injection, intraportal vein injection, intravenous injection, etc. Although theoretically, direct liver transfer of AAV would have the highest efficacy, this method requires more complicated processes including surgery and anaesthesia. Intravenous injection would be a more ingenious approach considering the time required and the risk of experimental variability. A standard adult mouse intravenous injection of AAV would be a delivery of 300–400μl injectate into the most accessible tail veins. The homeostatic and immunological responses of the mice would be closely monitored, in order to determine the optimal dose and volume of AAV injection. AAV with empty vectors would be used as control. The next step would be a measurement of transduction efficiency and specificity. Enzyme-linked immunosorbent assay (ELISA) would be applied to determine the NLVPMVATV expression level in tested and controlled tumor cells. The MHC class I NLVPMVATV presentation on tumor cells would be tested by detecting activation of NLVPMVATV-specific T cells. Single-cell RNA-sequencing would be adopted to measure the transcription level of the transfected NLVPMVATV and miRNA in major tissue types in order to determine the specificity. The data processing such as cell cluster identification would be done using the R package Seurat. We would collect information regarding the virus' biological characteristics and route of administration, as well as the replication competence, immunogenicity, persistence and latency, and tropism of the AAV. The mouse model would also be measured by relevant assays, in order to obtain the optimal dosage of virus injection. Our goal would be maximising the efficacy and specificity of transgene expression while minimizing cytokine storms. Before moving on to testing CAR-T, Kaplan–Meier survival analysis would be implemented in therapeutic and control mice. Tumor survival and growth will also be measured for two months.

CAR T cell engineering

NLVPMVATV-specific CAR T cells will be introduced after the AAV delivery has been optimized. Currently, CAR-T treatments are utilised for blood cancer treatment, whereas the CAR-T cells can locate and kill cancer cells simply through intravenous infusions. Although no CAR-T treatment has been approved for solid tumors, multiple clinical treatments were done targeting solid tumor genes. CAR-T cells targeting AFP have been used for the treatment of hepatocellular carcinoma in a phase 1 clinical trial. With regards to these clinical studies, intravenous infusions will also be adopted in our mouse models. After injection of CAR-T cells, the survival and growth of the tumor would be monitored by their size over 2 months. Kaplan-Meier survival analysis will be carried out again to compare the

therapeutic effect before and after administrating CAR-T. As the result is desirable in small tumors, we will move on to growing mouse models with larger tumor size. Most of the CAR-T cells used in the research field are shown to have low effectiveness in treating large solid tumors due to the difficulty in penetrating tumor tissues. The growth and survival of tumor, together with the survival rate of the mouse model will be recorded. In order to determine the efficacy of AAV and CAR-T infiltration in the tumor, we would test and compare relevant parameters, such as the number of cells and expression levels of transgenes, in core and peripheral tumor cells. The CAR-T killing effect will be accessed by detecting the luminescence activity of cells. The dose of CAR-T dose and the implementation timepoint after AAV administration will be optimised to maximise the cancer-killing ability and reduce side effects.

Reference

555. AAV vector-mediated efficient and sustained MIRNA antagonism in vivo for studying MIRNA function and treating hyperlipidemia. (2011). *Molecular Therapy*, *19*. https://doi.org/10.1016/s1525-0016(16)37128-3

Auricchio, A. (2003, April). Pseudotyped AAV vectors for constitutive and regulated gene expression in the eye. *Vision Research*, *43*(8), 913–918. https://doi.org/10.1016/s0042-6989(02)00676-4

Bai, D. S., Zhang, C., Chen, P., Jin, S. J., & Jiang, G. Q. (2017). The prognostic correlation of AFP level at diagnosis with pathological grade, progression, and survival of patients with hepatocellular carcinoma. *Scientific Reports*, *7*(1). https://doi.org/10.1038/s41598-017-12834-1

Bergamaschi, C., Pandit, H., Nagy, B. A., Stellas, D., Jensen, S. M., Bear, J., Cam, M., Valentin, A., Fox, B. A., Felber, B. K., & Pavlakis, G. N. (2020). Heterodimeric IL-15 delays tumor growth and promotes intratumoral CTL and dendritic cell accumulation by a cytokine network involving XCL1, IFN-γ, CXCL9 and CXCL10. *Journal for ImmunoTherapy of Cancer*, *8*(1). https://doi.org/10.1136/jitc-2020-000599

Bialecki, E. S., & di Bisceglie, A. M. (2005). Diagnosis of hepatocellular carcinoma. *HPB*, *7*(1), 26–34. https://doi.org/10.1080/13651820410024049

Boutin, S., Monteilhet, V., Veron, P., Leborgne, C., Benveniste, O., Montus, M. F., & Masurier, C. (2010, June). Prevalence of Serum IgG and Neutralizing Factors Against Adeno-Associated Virus (AAV) Types 1, 2, 5, 6, 8, and 9 in the Healthy Population: Implications for Gene Therapy Using AAV Vectors. *Human Gene Therapy*, *21*(6), 704–712. https://doi.org/10.1089/hum.2009.182

Brentjens, R. J., Davila, M. L., Riviere, I., Park, J., Wang, X., Cowell, L. G., Bartido, S., Stefanski, J., Taylor, C., Olszewska, M., Borquez-Ojeda, O., Qu, J., Wasielewska, T., He, Q., Bernal, Y., Rijo, I. V., Hedvat, C., Kobos, R., Curran, K., … Sadelain, M. (2013). CD19-targeted T cells rapidly induce molecular remissions in adults with chemotherapy-refractory acute lymphoblastic leukemia. Science Translational Medicine, 5(177). https://doi.org/10.1126/scitranslmed.3005930

Bubeník J. (2003). Tumor MHC class I downregulation and immunotherapy (Review). Oncology reports, 10(6), 2005–2008.

C. King, PharmD, BCOP, A., & S. Orozco, PharmD, J. (2019). Axicabtagene Ciloleucel: The first FDA-approved car T-cell therapy for relapsed/refractory large B-cell lymphoma. Journal of the Advanced Practitioner in Oncology, 10(8). https://doi.org/10.6004/jadpro.2019.10.8.9

Caliendo, F., Dukhinova, M., & Siciliano, V. (2019). Engineered cell-based therapeutics: Synthetic Biology Meets immunology. Frontiers in Bioengineering and Biotechnology, 7. https://doi.org/10.3389/fbioe.2019.00043

Center for Biologics Evaluation and Research. (2013). Preclinical Assessment of Investigational Cellular and Gene Therapy Products: Guidance for Industry. U.S. Food and Drug Administration. Retrieved June 14, 2022, from https://www.fda.gov/regulatory-information/search-fda-guidance-documents/preclinical-assessment-investigational-cellular-and-gene-therapy-products

Center for Biologics Evaluation and Research. (2015). Design and Analysis of Shedding Studies for Virus or Bacteria-Based Gene Therapy and Oncolytic Products: Guidance for Industry. U.S. Food and Drug Administration. Retrieved June 14, 2022, from https://www.fda.gov/regulatory-information/search-fda-guidance-documents/design-and-analysis-shedding-studies-virus-or-bacteria-based-gene-therapy-and-oncolytic-products

Chan, J. D., Scheidt, B., Zeng, B., Oliver, A. J., Davey, A. S., Ali, A. I., Thomas, R., Trapani, J. A., Darcy, P. K., Kershaw, M. H., Dolcetti, R., & Slaney, C. Y. (2020). Enhancing chimeric antigen receptor T-Cell Immunotherapy Against Cancer using a nanoemulsion-based vaccine targeting cross-presenting dendritic cells. Clinical & Translational Immunology, 9(7). https://doi.org/10.1002/cti2.1157

Cohen, A. D., Garfall, A. L., Stadtmauer, E. A., Melenhorst, J. J., Lacey, S. F., Lancaster, E., Vogl, D. T., Weiss, B. M., Dengel, K., Nelson, A., Plesa, G., Chen, F., Davis, M. M., Hwang, W.-T., Young, R. M., Brogdon, J. L., Isaacs, R., Pruteanu-Malinici, I., Siegel, D. L., … Milone, M. C. (2019). B cell maturation antigen–specific car T cells are clinically active in multiple myeloma. Journal of Clinical Investigation, 129(6), 2210–2221. https://doi.org/10.1172/jci126397

Cornel, A. M., Mimpen, I. L., & Nierkens, S. (2020). MHC Class I Downregulation in Cancer: Underlying Mechanisms and Potential Targets for Cancer Immunotherapy. Cancers, 12(7), 1760. https://doi.org/10.3390/cancers12071760

Davis JJ., Wang, L., Dong, F., Zhang, L., Guo, W., Teraishi, F., Xu, K., Ji, L., & Fang, B. (2006). Oncolysis and suppression of tumor growth by a GFP-expressing oncolytic adenovirus controlled by an hTERT and CMV hybrid promoter. Cancer Gene Therapy, 13(7), 720–723. https://doi.org/10.1038/sj.cgt.7700944

Expression of N4BP1 in cancer - summary - The human protein atlas. (n.d.). Retrieved March 8, 2022, from https://www.proteinatlas.org/ENSG00000102921-N4BP1/pathology

Fehlings, M. (2020). Faculty opinions recommendation of adeno-associated virus vector as a platform for gene therapy delivery. *Faculty Opinions – Post-Publication Peer Review of the Biomedical Literature*. https://doi.org/10.3410/f.734958350.793573257

Forloni, M., Albini, S., Limongi, M. Z., Cifaldi, L., Boldrini, R., Nicotra, M. R., Giannini, G., Natali, P. G., Giacomini, P., & Fruci, D. (2010). NF-kappaB, and not MYCN, regulates MHC class I and endoplasmic reticulum aminopeptidases in human neuroblastoma cells. Cancer research, 70(3), 916–924. https://doi.org/10.1158/0008-5472.CAN-09-2582

Forterre, A., Komuro, H., Aminova, S., & Harada, M. (2020). A Comprehensive Review of Cancer MicroRNA Therapeutic Delivery Strategies. Cancers, 12(7), 1852. https://doi.org/10.3390/cancers12071852

Fry, T. J., Shah, N. N., Orentas, R. J., Stetler-Stevenson, M., Yuan, C. M., Ramakrishna, S., Wolters, P., Martin, S., Delbrook, C., Yates, B., Shalabi, H., Fountaine, T. J., Shern, J. F., Majzner, R. G., Stroncek, D. F., Sabatino, M., Feng, Y., Dimitrov, D. S., Zhang, L., … Mackall, C. L. (2017). CD22-targeted car T cells induce remission in B-all that is naive or resistant to CD19-targeted car immunotherapy. Nature Medicine, 24(1), 20–28. https://doi.org/10.1038/nm.4441

Gao Z.L., Herrera-Carrillo, E., & Berkhout, B. (2018). RNA Polymerase II Activity of Type 3 Pol III Promoters. Molecular Therapy. Nucleic Acids, 12, 135–145. https://doi.org/10.1016/j.omtn.2018.05.001

Grada, Z., Hegde, M., Byrd, T., Shaffer, D. R., Ghazi, A., Brawley, V. S., Corder, A., Schönfeld, K., Koch, J., Dotti, G., Heslop, H. E., Gottschalk, S., Wels, W. S., Baker, M. L., & Ahmed, N. (2013). Tancar: A novel bispecific chimeric antigen receptor for cancer immunotherapy. Molecular Therapy - Nucleic Acids, 2. https://doi.org/10.1038/mtna.2013.32

Grosskopf, A. K., Labanieh, L., Klysz, D. D., Roth, G. A., Xu, P., Adebowale, O., Gale, E. C., Jons, C. K., Klich, J. H., Yan, J., Maikawa, C. L., Correa, S., Ou, B. S., d'Aquino, A. I., Cochran, J. R., Chaudhuri, O., Mackall, C. L., & Appel, E. A. (2022). Delivery of car-T cells in a transient injectable stimulatory hydrogel niche improves treatment of solid tumors. Science Advances, 8(14). https://doi.org/10.1126/sciadv.abn8264

Guo, P., Yu, C., Wang, Q., Zhang, R., Meng, X., & Feng, Y. (2018, June). Liposome Lipid-Based Formulation Has the Least Influence on rAAV Transduction Compared to Other Transfection Agents. *Molecular Therapy - Methods &Amp; Clinical Development*, *9*, 367–375. https://doi.org/10.1016/j.omtm.2018.04.004

Halliday, G. M., Patel, A., Hunt, M. J., Tefany, F. J., & Barnetson, R. S. (1995). Spontaneous regression of human melanoma/nonmelanoma skin cancer: Association with infiltrating CD4+ T cells. World Journal of Surgery, 19(3), 352–358. https://doi.org/10.1007/bf00299157

Hao, Y., Hao, S., Andersen-Nissen, E., Mauck, W. M., Zheng, S., Butler, A., Lee, M. J., Wilk, A. J., Darby, C., Zager, M., Hoffman, P., Stoeckius, M., Papalexi, E., Mimitou, E. P., Jain, J., Srivastava, A., Stuart, T., Fleming, L. M., Yeung, B., … Satija, R. (2021). Integrated Analysis of multimodal single-cell data. Cell, 184(13). https://doi.org/10.1016/j.cell.2021.04.048

Haug, M., Brede, G., Håkerud, M., Nedberg, A. G., Gederaas, O. A., Flo, T. H., Edwards, V. T., Selbo, P. K., Høgset, A., & Halaas, Ø. (2018). Photochemical internalization of peptide antigens provides a novel strategy to realize therapeutic cancer vaccination. Frontiers in Immunology, 9. https://doi.org/10.3389/fimmu.2018.00650

Hu, X., Chen, R., Wei, Q., & Xu, X. (2022). The Landscape Of Alpha Fetoprotein In Hepatocellular Carcinoma: Where Are We? *International Journal of Biological Sciences*, *18*(2), 536–551. https://doi.org/10.7150/ijbs.64537

Hüser, D., Gogol-Döring, A., Lutter, T., Weger, S., Winter, K., Hammer, E.-M., Cathomen, T., Reinert, K., & Heilbronn, R. (2010). Integration preferences of wildtype AAV-2 for consensus rep-binding sites at numerous loci in the human genome. *PLoS Pathogens*, *6*(7). https://doi.org/10.1371/journal.ppat.1000985

Johnson, C., Han, Y., Hughart, N., McCarra, J., Alpini, G., & Meng, F. (2012). Interleukin-6 and its receptor, key players in hepatobiliary inflammation and cancer. Psychologia Latina, 1(1), 58-70.

K.R. Parker, D. Migliorini, E. Perkey, K.E. Yost, A. Bhaduri, P. Bagga, M. Haris, N.E. Wilson, F. L iu, K. Gabunia, J. Scholler, T.J. Montine, V.G. Bhoj, R. Reddy, S. Mohan, I. Maillard, A.R. Krieg stein, C.H. June, H.Y. Chang, A.D. Posey Jr., A.T. Satpathy

Kanazawa, T., Mizukami, H., Okada, T., Hanazono, Y., Kume, A., Nishino, H., Takeuchi, K., Kitamura, K., Ichimura, K., & Ozawa, K. (2003). Suicide gene therapy using AAV-HSVTK/ganciclovir in combination with irradiation results in regression of human head and neck cancer xenografts in Nude mice. Gene Therapy, 10(1), 51–58. https://doi.org/10.1038/sj.gt.3301837

Kang, T. H., Ma, B., Wang, C., Wu, T. C., & Hung, C. F. (2013). Targeted Coating With Antigenic Peptide Renders Tumor Cells Susceptible to CD8+ T Cell-mediated Killing. *Molecular Therapy*, *21*(3), 542–553. https://doi.org/10.1038/mt.2012.233

Kang, T. H., Ma, B., Wang, C., Wu, T.-C., & Hung, C.-F. (2013). Targeted coating with antigenic peptide renders tumor cells susceptible to CD8+ T cell-mediated killing. Molecular Therapy, 21(3), 542–553. https://doi.org/10.1038/mt.2012.233

Karandikar, S. H., Sidney, J., Sette, A., Selby, M. J., Korman, A. J., & Srivastava, P. K. (2019). Identification of epitopes in ovalbumin that provide insights for cancer neoepitopes. *JCI Insight*, *4*(8). https://doi.org/10.1172/jci.insight.127882

Ke, Y., Li, Y., & Kapp, J. A. (1995). Ovalbumin injected with complete Freund's adjuvant stimulates cytolytic responses. European Journal of Immunology, 25(2), 549–553. https://doi.org/10.1002/eji.1830250237

Keswani, S. G., Balaji, S., Le, L., Leung, A., Lim, F. Y., Habli, M., Jones, H. N., Wilson, J. M., & Crombleholme, T. M. (2012, June 19). Pseudotyped adeno-associated viral vector tropism and transduction efficiencies in murine wound healing. *Wound Repair and Regeneration*, n/a-n/a. https://doi.org/10.1111/j.1524-475x.2012.00810.x

Kim, J. H., Lee, S. R., Li, L. H., Park, H. J., Park, J. H., Lee, K. Y., Kim, M. K., Shin, B. A., & Choi, S. Y. (2011). High Cleavage Efficiency of a 2A Peptide Derived from Porcine Teschovirus-1 in

Human Cell Lines, Zebrafish and Mice. *PLoS ONE*, *6*(4), e18556. https://doi.org/10.1371/journal.pone.0018556

Kota J, Chivukula RR, O'Donnell KA, et al. Therapeutic microRNA delivery suppresses tumorigenesis in a murine liver cancer model. Cell. 2009;137(6):1005–1017.
Li, C., Hirsch, M., DiPrimio, N., Asokan, A., Goudy, K., Tisch, R., & Samulski, R. J. (2009, July). Cytotoxic-T-Lymphocyte-Mediated Elimination of Target Cells Transduced with Engineered Adeno-Associated Virus Type 2 Vector In Vivo. *Journal of Virology*, *83*(13), 6817–6824. https://doi.org/10.1128/jvi.00278-09

Li, X.-an. (2017). A Clinical Research of CAR T Cells Targeting EpCAM Positive Cancer (CARTEPC). A Clinical Research of CAR T Cells Targeting EpCAM Positive Cancer - ClinicalTrials.gov. Retrieved Sept 14, 2022, from https://clinicaltrials.gov/ct2/show/NCT03013712

Linden, R. M., Winocour, E., & Berns, K. I. (1996). The recombination signals for adeno-associated virus site-specific integration. *Proceedings of the National Academy of Sciences*, *93*(15), 7966–7972. https://doi.org/10.1073/pnas.93.15.7966

Liu, Z., Chen, O., Wall, J. B. J., Zheng, M., Zhou, Y., Wang, L., Ruth Vaseghi, H., Qian, L., & Liu, J. (2017). Systematic comparison of 2A peptides for cloning multi-genes in a polycistronic vector. *Scientific Reports*, *7*(1). https://doi.org/10.1038/s41598-017-02460-2

Lu, Y., Zhu, M., Li, W., Lin, B., Dong, X., Chen, Y., Xie, X., Guo, J., & Li, M. (2016). Alpha fetoprotein plays a critical role in promoting metastasis of hepatocellular carcinoma cells. *Journal of Cellular and Molecular Medicine*, *20*(3), 549–558. https://doi.org/10.1111/jcmm.12745

Majzner, R. G., Rietberg, S. P., Labanieh, L., Sotillo, E., Weber, E. W., Lynn, R. C., Theruvath, J. L., Yuan, C. M., Xu, P., Nguyen, S. M., Shah, N. N., Stetler-Stevenson, M., Fry, T. J., Lee, D. W., & Mackall, C. L. (2018). Low CD19 antigen density diminishes efficacy of CD19 car T cells and can be overcome by rational redesign of car signaling domains. Blood, 132(Supplement 1), 963–963. https://doi.org/10.1182/blood-2018-99-115558

Mardiana, S., Shestova, O., Ruella, M., & Gill, S. (2020). Repurposing bi-specific chimeric antigen receptor (CAR) approach to enhance car T cell activity against low antigen density tumors. Blood, 136(Supplement 1), 30–30. https://doi.org/10.1182/blood-2020-140092

Marofi, F., Motavalli, R., Safonov, V. A., Thangavelu, L., Yumashev, A. V., Alexander, M., Shomali, N., Chartrand, M. S., Pathak, Y., Jarahian, M., Izadi, S., Hassanzadeh, A., Shirafkan, N., Tahmasebi, S., & Khiavi, F. M. (2021). Car T cells in solid tumors: Challenges and opportunities. Stem Cell Research & Therapy, 12(1). https://doi.org/10.1186/s13287-020-02128-1

Marofi, F., Motavalli, R., Safonov, V. A., Thangavelu, L., Yumashev, A. V., Alexander, M., Shomali, N., Chartrand, M. S., Pathak, Y., Jarahian, M., Izadi, S., Hassanzadeh, A., Shirafkan, N., Tahmasebi, S., & Khiavi, F. M. (2021). Car T cells in solid tumors: Challenges and

opportunities. Stem Cell Research & Therapy, 12(1). https://doi.org/10.1186/s13287-020-02128-1

Meumann, N., Schmithals, C., Elenschneider, L., Hansen, T., Balakrishnan, A., Hu, Q., Hook, S., Schmitz, J., Bräsen, J. H., Franke, A.-C., Olarewaju, O., Brandenberger, C., Talbot, S. R., Fangmann, J., Hacker, U. T., Odenthal, M., Ott, M., Piiper, A., & Büning, H. (2022). Hepatocellular carcinoma is a natural target for adeno-associated virus (AAV) 2 vectors. *Cancers*, *14*(2), 427. https://doi.org/10.3390/cancers14020427

Meumann, N., Schmithals, C., Elenschneider, L., Hansen, T., Balakrishnan, A., Hu, Q., Hook, S., Schmitz, J., Bräsen, J. H., Franke, A. C., Olarewaju, O., Brandenberger, C., Talbot, S. R., Fangmann, J., Hacker, U. T., Odenthal, M., Ott, M., Piiper, A., & Büning, H. (2022, January 15). Hepatocellular Carcinoma Is a Natural Target for Adeno-Associated Virus (AAV) 2 Vectors. *Cancers*, *14*(2), 427. https://doi.org/10.3390/cancers14020427

Mikucki, M. E., Fisher, D. T., Matsuzaki, J., Skitzki, J. J., Gaulin, N. B., Muhitch, J. B., Ku, A. W., Frelinger, J. G., Odunsi, K., Gajewski, T. F., Luster, A. D., & Evans, S. S. (2015).
Mizuguchi, H., Xu, Z., Ishii-Watabe, A., Uchida, E., & Hayakawa, T. (2000). IRES-dependent second gene expression is significantly lower than cap-dependent first gene expression in a bicistronic vector. *Molecular Therapy*, *1*(4), 376–382. https://doi.org/10.1006/mthe.2000.0050

Mojic M, Takeda K, Hayakawa Y. The Dark Side of IFN-γ: Its Role in Promoting Cancer Immunoevasion. Int J Mol Sci. 2017;19(1):89. Published 2017 Dec 28. doi:10.3390/ijms19010089

Montaño-Samaniego, M., Bravo-Estupiñan, D. M., Méndez-Guerrero, O., Alarcón-Hernández, E., & Ibáñez-Hernández, M. (2020). Strategies for targeting gene therapy in cancer cells with tumor-specific promoters. *Frontiers in Oncology*, *10*. https://doi.org/10.3389/fonc.2020.605380

Morgan, R. A., Yang, J. C., Kitano, M., Dudley, M. E., Laurencot, C. M., & Rosenberg, S. A. (2010). Case report of a serious adverse event following the administration of T cells transduced with a chimeric antigen receptor recognizing ERBB2. Molecular Therapy, 18(4), 843–851. https://doi.org/10.1038/mt.2010.24

Nagarsheth, N., Wicha, M. S., & Zou, W. (2017). Chemokines in the cancer microenvironment and their relevance in cancer immunotherapy. Nature Reviews Immunology, 17(9), 559–572. https://doi.org/10.1038/nri.2017.49

Nawy, T. (2013). Single-cell sequencing. Nature Methods, 11(1), 18–18. https://doi.org/10.1038/nmeth.2771

Nepravishta, R., Ferrentino, F., Mandaliti, W., Mattioni, A., Weber, J., Polo, S., Castagnoli, L., Cesareni, G., Paci, M., & Santonico, E. (2019). CoCUN, a Novel Ubiquitin Binding Domain Identified in N4BP1. Biomolecules, 9(7), 284. https://doi.org/10.3390/biom9070284

Ningarhari, M., Caruso, S., Hirsch, T. Z., Bayard, Q., Franconi, A., Védie, A. L., Noblet, B., Blanc, J. F., Amaddeo, G., Ganne, N., Ziol, M., Paradis, V., Guettier, C., Calderaro, J., Morcrette, G., Kim, Y., MacLeod, A. R., Nault, J. C., Rebouissou, S., & Zucman-Rossi, J. (2021). Telomere length is key to hepatocellular carcinoma diversity and telomerase addiction is an actionable therapeutic target. Journal of Hepatology, 74(5), 1155–1166. https://doi.org/10.1016/j.jhep.2020.11.052

Ningarhari, M., Caruso, S., Hirsch, T. Z., Bayard, Q., Franconi, A., Védie, A. L., Noblet, B., Blanc, J. F., Amaddeo, G., Ganne, N., Ziol, M., Paradis, V., Guettier, C., Calderaro, J., Morcrette, G., Kim, Y., MacLeod, A. R., Nault, J. C., Rebouissou, S., & Zucman-Rossi, J. (2021). Telomere length is key to hepatocellular carcinoma diversity and telomerase addiction is an actionable therapeutic target. Journal of Hepatology, 74(5), 1155–1166. https://doi.org/10.1016/j.jhep.2020.11.052

Non-redundant requirement for CXCR3 signalling during tumoricidal T-cell trafficking across tumor vascular checkpoints. Nature Communications, 6(1). https://doi.org/10.1038/ncomms8458

Nowrouzi, A., Penaud-Budloo, M., Kaeppel, C., Appelt, U., Le Guiner, C., Moullier, P., Kalle, C. von, Snyder, R. O., & Schmidt, M. (2012). Integration frequency and intermolecular recombination of Raav vectors in non-human primate skeletal muscle and liver. *Molecular Therapy*, *20*(6), 1177–1186. https://doi.org/10.1038/mt.2012.47

O'Rourke, D. M., Nasrallah, M. L. P., Desai, A., Melenhorst, J. J., Mansfield, K., Morrissette, J. J., Martinez-Lage, M., Brem, S., Maloney, E., Shen, A., Isaacs, R., Mohan, S., Plesa, G., Lacey, S. F., Navenot, J.-M., Zheng, Z., Levine, B. L., Okada, H., June, C. H., … Maus, M. V. (2017). A single dose of peripherally infused EGFRVIII-directed car T cells mediates antigen loss and induces adaptive resistance in patients with recurrent glioblastoma. Science Translational Medicine, 9(399). https://doi.org/10.1126/scitranslmed.aaa0984

Olson, B., Li, Y., Lin, Y., Liu, E. T., & Patnaik, A. (2018). Mouse models for Cancer Immunotherapy Research. Cancer Discovery, 8(11), 1358–1365. https://doi.org/10.1158/2159-8290.cd-18-0044

Park, A. K., Fong, Y., Kim, S.-I., Yang, J., Murad, J. P., Lu, J., Jeang, B., Chang, W.-C., Chen, N. G., Thomas, S. H., Forman, S. J., & Priceman, S. J. (2020). Effective combination immunotherapy using oncolytic viruses to deliver car targets to solid tumors. Science Translational Medicine, 12(559). https://doi.org/10.1126/scitranslmed.aaz1863

Qian, Q., Jin, H., Zhang, Z., Sun, Y., & Wang, J. (2017, June 7). CTLA-4 and PD-1 Antibodies Expressing MUC1-CAR-T Cells for MUC1 Positive Advanced Solid Tumor. CTLA-4 and PD-1 Antibodies Expressing MUC1-CAR-T Cells for MUC1 Positive Advanced Solid Tumor - ClinicalTrials.gov. Retrieved June 14, 2022, from https://clinicaltrials.gov/ct2/show/NCT03179007

Reed, S. E., Staley, E. M., Mayginnes, J. P., Pintel, D. J., & Tullis, G. E. (2006, December). Transfection of mammalian cells using linear polyethylenimine is a simple and effective means of producing recombinant adeno-associated virus vectors. *Journal of Virological Methods*, *138*(1–2), 85–98. https://doi.org/10.1016/j.jviromet.2006.07.024

Richman, S. A., Nunez-Cruz, S., Moghimi, B., Li, L. Z., Gershenson, Z. T., Mourelatos, Z., Barrett, D. M., Grupp, S. A., & Milone, M. C. (2018). High-affinity GD2-specific car T cells induce fatal encephalitis in a preclinical neuroblastoma model. Cancer Immunology Research, 6(1), 36–46. https://doi.org/10.1158/2326-6066.cir-17-0211

Ronzitti, G., Gross, D.-A., & Mingozzi, F. (2020). Human immune responses to adeno associated virus (AAV) vectors. *Frontiers in Immunology*, *11*. https://doi.org/10.3389/fimmu.2020.00670

Rötzschke, O., Falk, K., Stevanovic, S., Jung, G., Walden, P., & Rammensee, H.-G. (1991). Exact prediction of a natural T cell epitope. European Journal of Immunology, 21(11), 2891–2894. https://doi.org/10.1002/eji.1830211136

Sands, M. S. (2011). Aav-mediated liver-directed gene therapy. Adeno-Associated Virus, 141–157. https://doi.org/10.1007/978-1-61779-370-7_6
Santiago-Ortiz, J. L., & Schaffer, D. V. (2016). Adeno-associated virus (AAV) vectors in cancer gene therapy. Journal of Controlled Release, 240, 287–301. https://doi.org/10.1016/j.jconrel.2016.01.001

Siegler, E. L., & Wang, P. (2018). Preclinical models in chimeric antigen receptor–engineered T-cell therapy. Human Gene Therapy, 29(5), 534–546. https://doi.org/10.1089/hum.2017.243

Single-cell analyses identify brain mural cells expressing CD19 as potential off-tumor targets for CAR-T immunotherapies
Song, Q. (2017). Clinical study of ET1402L1-car T cells in AFP expressing hepatocellular carcinoma - full text view. Clinical Study of ET1402L1-CAR T Cells in AFP Expressing Hepatocellular Carcinoma - ClinicalTrials.gov. Retrieved June 14, 2022, from https://clinicaltrials.gov/ct2/show/NCT03349255

Spiegel, J. Y., Patel, S., Muffly, L., Hossain, N. M., Oak, J., Baird, J. H., Frank, M. J., Shiraz, P., Sahaf, B., Craig, J., Iglesias, M., Younes, S., Natkunam, Y., Ozawa, M. G., Yang, E., Tamaresis, J., Chinnasamy, H., Ehlinger, Z., & Miklos, D. B. (2019). Modified immune cells (CD19-CD22 car T cells) in treating patients with recurrent or refractory CD19 positive, CD22 positive leukemia or lymphoma. Case Medical Research. https://doi.org/10.31525/ct1-nct04029038

Tang, Li, Y., Ma, J., Wang, X., Zhao, W., Hossain, M. A., & Yang, Y. (2020). Adenovirus-mediated specific tumor tagging facilitates CAR-T therapy against antigen-mismatched solid tumors. Cancer Letters, 487, 1–9. https://doi.org/10.1016/j.canlet.2020.05.013

Team:BGU Israel—2015.igem.org. (n.d.). Retrieved Sept 11, 2022, from https://2015.igem.org/Team:BGU_Israel

Team:CPU CHINA - 2018.igem.org. (n.d.). Retrieved Sept 11, 2022, from https://2018.igem.org/Team:CPU_CHINA

Team:CSU CHINA - 2019.igem.org. (n.d.). Retrieved Sept 11, 2022, from https://2019.igem.org/Team:CSU_CHINA

Team:Evry—2015.igem.org. (n.d.). Retrieved Sept 11, 2022, from https://2015.igem.org/Team:Evry

Team:Nanjing NFLS - 2019.igem.org. (n.d.). Retrieved Sept 11, 2022, from https://2019.igem.org/Team:Nanjing_NFLS

Tsukamoto, H., Fujieda, K., Senju, S., Ikeda, T., Oshiumi, H., & Nishimura, Y. (2017). Immune-suppressive effects of interleukin-6 on T-cell-mediated anti-tumor immunity. *Cancer Science*, *109*(3), 523–530. https://doi.org/10.1111/cas.13433

Vargas, J. E., Chicaybam, L., Stein, R. T., Tanuri, A., Delgado-Cañedo, A., & Bonamino, M. H. (2016). Retroviral vectors and transposons for stable gene therapy: Advances, current challenges and perspectives. *Journal of Translational Medicine*, *14*(1). https://doi.org/10.1186/s12967-016-1047-x

Waldman, A. D., Fritz, J. M., & Lenardo, M. J. (2020). A guide to cancer immunotherapy: From T cell basic science to clinical practice. Nature Reviews Immunology, 20(11), 651–668. https://doi.org/10.1038/s41577-020-0306-5

Wang, Y., Wang, F., Wang, R., Zhao, P., & Xia, Q. (2015). 2A self-cleaving peptide-based multi-gene expression system in the silkworm Bombyx mori. *Scientific Reports*, *5*(1). https://doi.org/10.1038/srep16273

Wright, J. F. (2009, July). Transient Transfection Methods for Clinical Adeno-Associated Viral Vector Production. *Human Gene Therapy*, *20*(7), 698–706. https://doi.org/10.1089/hum.2009.064

Wu, X., Luo, H., Shi, B., Di, S., Sun, R., Su, J., Liu, Y., Li, H., Jiang, H., & Li, Z. (2019). Combined antitumor effects of sorafenib and GPC3-car T cells in mouse models of hepatocellular carcinoma. Molecular Therapy, 27(8), 1483–1494. https://doi.org/10.1016/j.ymthe.2019.04.020

Yang, X., Liang, L., Zhang, X.-F., Jia, H.-L., Qin, Y., Zhu, X.-C., Gao, X.-M., Qiao, P., Zheng, Y., Sheng, Y.-Y., Wei, J.-W., Zhou, H.-J., Ren, N., Ye, Q.-H., Dong, Q.-Z., & Qin, L.-X. (2013). MicroRNA-26A suppresses tumor growth and metastasis of human hepatocellular carcinoma by targeting interleukin-6-stat3 pathway. *Hepatology*, *58*(1), 158–170. https://doi.org/10.1002/hep.26305

Yu, J. I., Choi, C., Ha, S. Y., Park, C. K., Kang, S. Y., Joh, J. W., Paik, S. W., Kim, S., Kim, M., Jung, S. H., & Park, H. C. (2017). Clinical importance of TERT overexpression in hepatocellular

carcinoma treated with curative surgical resection in HBV endemic area. Scientific Reports, 7(1). https://doi.org/10.1038/s41598-017-12469-2

Zhang, W., Moore, L., & Ji, P. (2011). Mouse models for cancer research. Chinese Journal of Cancer, 30(3), 149–152. https://doi.org/10.5732/cjc.011.10047

Zhou, S.-L., Hu, Z.-Q., Zhou, Z.-J., Dai, Z., Wang, Z., Cao, Y., Fan, J., Huang, X.-W., & Zhou, J. (2016). Mir-28-5p-il-34-macrophage feedback loop modulates hepatocellular carcinoma metastasis. Hepatology, 63(5), 1560–1575. https://doi.org/10.1002/hep.28445